ELECTRICAL ENGINEERING RESEARCH LABORATORY
THE UNIVERSITY OF TEXAS
Austin, Texas

QUARTERLY ENGINEERING REPORT NO. 5

PART I

A SPECTROSCOPIC MEASUREMENT OF THE RESONANT ABSORPTION OF MICROWAVE ENERGY BY OXYGEN IN THE 2.5-MILLIMETER WAVELENGTH REGION

by

A. E. Schulze

Contract AF 33(657)-8716
Project 4062

Aeronautical Systems Division
AIR FORCE SYSTEMS COMMAND
Wright-Patterson Air Force Base, Ohio

PART I

TABLE OF CONTENTS

		Page
	LIST OF FIGURES	iii
	ABSTRACT	iv
I.	INTRODUCTION	1
II.	ELEMENTS OF MICROWAVE SPECTROSCOPY	7
III.	THE OXYGEN MOLECULE: SPECTROSCOPIC ACTIVITY IN THE MICROWAVE REGION	18
IV.	STATEMENT OF THE PROBLEM	20
V.	INSTRUMENTATION	21
	A. Elements of a Microwave Spectrometer	21
	B. Types of Microwave Spectrometers	22
	C. The Design of a Spectrometer for this Investigation	25
VI.	TECHNIQUES OF MEASUREMENT	40
	A. Dynamic-Frequency Techniques	40
	B. Static-Frequency Techniques	41
	C. Operational Intricacies	42
VII.	THE DATA	45
VIII.	DISCUSSION AND ANALYSIS OF DATA	53
IX.	CONCLUSIONS	64
	BIBLIOGRAPHY	65
	APPENDICES	
	A. Calculations of Doppler Broadening and Wall-Collision Broadening of Line Width	
	B. Antenna Placement Calculations	
	C. Calibration of Sinusoidal Frequency Scale	

PART I

LIST OF FIGURES

Fig. No.	Title	Page No.
1	Calculated oxygen and water vapor attenuation of the earth's atmosphere for the millimeter wavelength spectrum	3
2	The 500-foot long, 6-inch diameter, absorption cell	27
3	Block diagram of spectrometer	33
4	The pressure gauges, oxygen bottles, and associated cell-pressurinzing equipment	36
5	The receiver viewed from the receiving end of the absorption cell	37
6	A close-up view of the receiver	38
7	The transmitter	39
8	Samples of oxygen absorption data obtained by use of spectrometer	44
9	Attenuation versus frequency for pressures of 700, 500, and 300 millimeters of mercury	46
10	Attenuation versus frequency for pressures of 760, 600, and 200 millimeters of mercury	47
11	Attenuation versus frequency for pressures of 30, 15, and 8 millimeters of mercury	48
12	Half-intensity, half-width of line versus pressure	49
13	Peak intensity of line versus pressure	50
14	Half-intensity, half-width of line versus pressure for low pressures	51
15	Peak intensity of line versus pressure for low pressures	52

PART I

ABSTRACT

The quest for broad-bandwidth communications channels has led to the investigation of the propagation of radio signals in the 10^{11} to 10^{12} cps frequency range where the absorption of energy by oxygen and water vapor makes the atmosphere partially opaque. A microwave spectrometer, described in this report, was used to measure the dependence of the oxygen component of absorption in the vicinity of 118.75 Gc.

The variations of line shape, both width and intensity, for a wide range of atmospheric pressures are described by the reported measurements. For 100% oxygen at a temperature of 300°K, the measurements, associated with the best fit of the Van Vleck-Weisskopf shape, yield a line-width parameter of $\frac{\Delta\nu}{P}$ = 2.08 Mc/mm Hg for $P \leqq 4$ mm Hg and $\frac{\Delta\nu}{P}$ = 1.90 Mc/mm Hg for 4 mm Hg for $P \leq 760$ mm Hg, and a peak intensity which increases very slightly with pressure from 6.5 db/km at 3.5 mm Hg to 7.0 db/km at 500 to 760 mm Hg.

I. INTRODUCTION

In compliance with the consistently increasing demands for broad bandwidth communications channels in the electromagnetic spectrum for the transmission of increasing amounts of information, the upper limit of the range of usable communications frequencies has been dramatically extended during the past decade. Where it was previously adequate to describe the wavelengths of the usable frequencies in terms of kilometers and meters, it is now necessary to use the terms centimeters, millimeters, and even microns. The use of shorter wavelengths makes terms such as "gigacycles" and "teracycles" expedient when frequencies are described. Thus, scientists and engineers, especially over the past two decades, have been vitally and actively concerned with the generation, as well as the propagation, of coherent electromagnetic radiation of increasingly higher frequencies.

Propagation of signals in the millimeter radio spectrum, signals of one-centimeter to one-millimeter wavelengths, through the atmosphere of the earth involves obstacles which are absent or negligible at the lower frequencies. Radiation of these frequencies is selectively attenuated due to the resonant absorption of energy by the gaseous constituents of the atmosphere. Although many gases have resonances in this region of the spectrum, the largest components of absorption arise from the constituent gases with the largest density.

The total atmospheric absorption of energy of millimeter wavelengths is the sum of the resonant attenuation of selected wavelengths by free molecules of uncondensed gases and the attenuation due to solid particles which are suspended in the gases. Problems associated with determining the physical size and distribution of solid particles suspended in the atmosphere make the component of attenuation due to these particles difficult to predict. However, the component of attenuation due to the resonant absorption of energy by the gaseous constituents of the atmosphere, which is usually the larger component, is mathematically predictable using a quantum-mechanical molecular model. Although the resonant component of attenuation can be measured by several different methods, [9, 19, 25, 27*] the problem is essentially one within the area of study termed "microwave spectroscopy."

Of the principal uncondensed atmospheric gases, only oxygen and water vapor have the molecular properties necessary for interaction with electromagnetic energy in the portion of the spectrum between wavelengths of one centimeter and one millimeter. From Figure 1, [26] it is evident that oxygen absorption makes the atmosphere "opaque" for a band of wavelengths centered at approximately five millimeters and for a narrow band centered at 2.53 millimeters. Water vapor absorption in this region of the spectrum is due largely to the "wings" of the water vapor absorption in the infrared and submillimeter regions; however, there is an absorption maximum

---

* Superscript numerals refer to the numbered references in the bibliography. A letter suffix identifies the location of the topic within the reference.

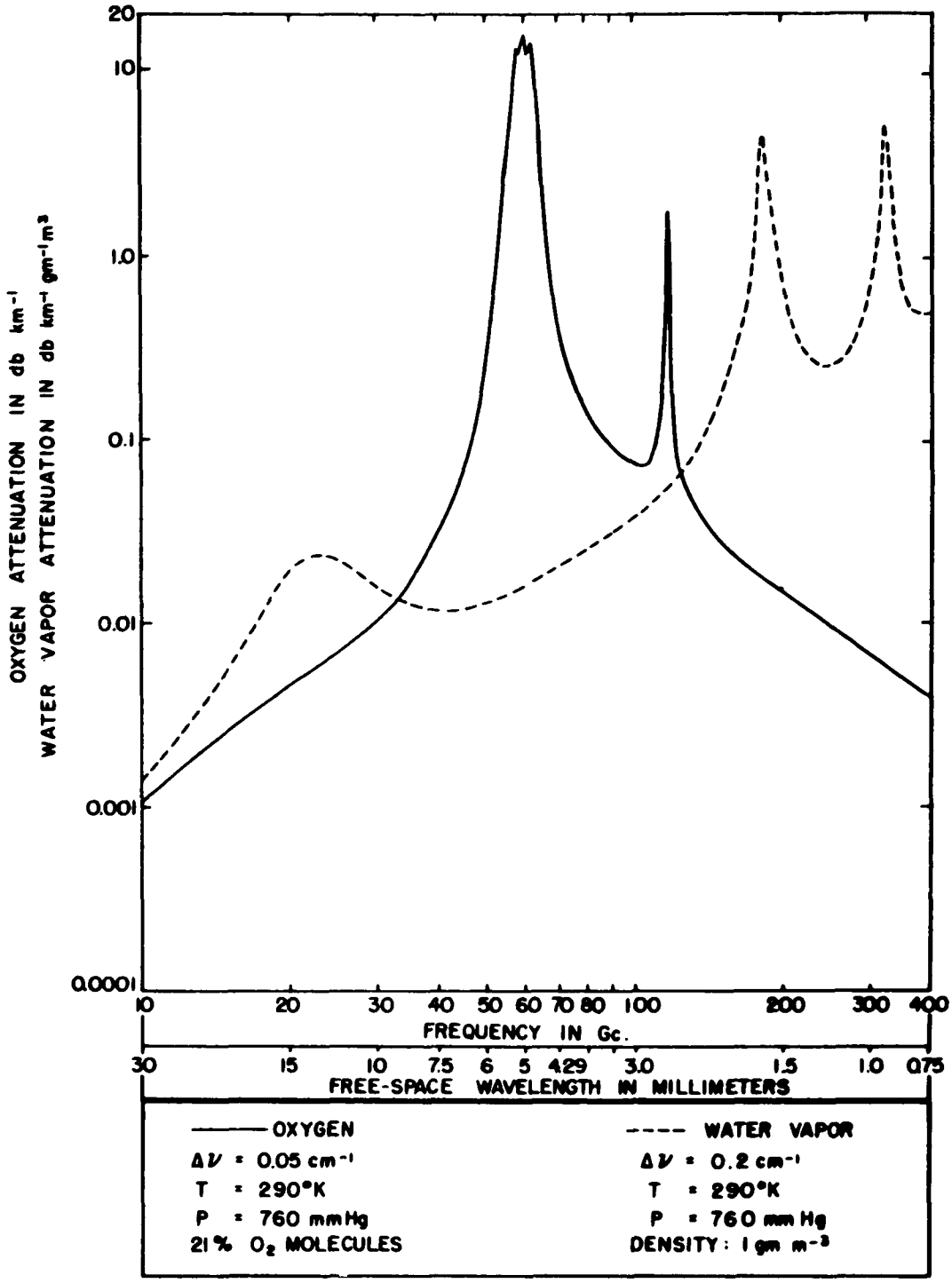

CALCULATED OXYGEN AND WATER VAPOR ATTENUATION OF THE EARTH'S ATMOSPHERE FOR THE MILLIMETER WAVELENGTH SPECTRUM

FIG. 1.

attributed to water vapor in the vicinity of 1.6 millimeters.

The summation of attenuation due to oxygen and water vapor produces several attenuation maxima and minima in the millimeter spectrum. The shape and opacity of the attenuation minima or "windows" are dependent upon the pressure, the temperature, and the molecular density of the gases. The oxygen absorption maximum centered at 2.53-millimeter wavelength separates two of these windows; hence, it is important to know the shape and intensity of the oxygen absorption at various atmospheric pressures in order that the effect of this component of absorption upon the shape of these two windows may be determined.

The absorption of five-millimeter wavelength energy by oxygen has been shown to be due to a multiplicity of spectral absorption lines* of the oxygen molecule which are resolved only at very low pressures. Theory has predicted the single spectral line of oxygen near 118.75 Gc,[29a] but measurements of this spectral line have been delayed by the state of the art of producing coherent electromagnetic radiation of this frequency and by the experimental difficulties associated with the short wavelengths. Energy sources of sufficient stability and coherence to permit these measurements have just recently been developed.

---

* The ideal absorption of energy at only a single frequency has caused the effect to be called a "spectral line." Since the width of any actual spectral line is usually small compared with its resonant frequency, the term "line" is actually very descriptive.

Interest in the propagation of energy at these extremely short wavelengths has been stimulated by the discovery that millimeter waves penetrate a plasma similar to the plasma sheath surrounding a space capsule during re-entry and, thus, comprise a possible solution to the "blackout" in communications with the capsule during this critical period. Quantitative information on the shape and intensity of the oxygen absorption lines can also be used to calibrate radio telescopes, both for obtaining information on the amount of oxygen found in the atmospheres of other planets and for operating at the frequencies of the windows. The shape and intensity of the oxygen lines can be used to provide detailed information on the molecular structure of the oxygen molecule itself. Other possible applications of oxygen absorption include the development of secret communications systems for communicating between space vehicles with atmospheric absorption preventing the interception of the signals on earth, methods of non-destructive testing and chemical analyses, and methods of constructing high-precision frequency standards.

Since the 2.53-millimeter oxygen absorption maximum is due to a single oxygen line, measurements of the shape of this line should contain a minimum of interference from other major oxygen spectral lines. Hence, this line should provide a maximum of line-shape information for verifying or refuting the mathematical model of the line. Mathematical formulas describing the line shape obtained from such measurements have possible

applications in the analysis of the closely-spaced oxygen lines in the 60 Gc region.

Before decisions can be made in the design of the instrumentation to acquire the data of this research project, the critical elements involved in the measurements, the accuracy required of the data, and the methods used by other researchers for similar investigations must be understood. A knowledge of microwave spectroscopy is basic to such an understanding.

II. ELEMENTS OF MICROWAVE SPECTROSCOPY

With the experiments of Cleeton and Williams[8] in 1934, a new branch of spectroscopy began involving that portion of the electromagnetic spectrum which lies in the microwave region. The development of reasonably monochromatic microwave signal sources during World War II led to renewed and intensified interest in the subject and paved the way for the development of modern microwave spectrometers.

Microwave spectroscopy is similar to spectroscopy in other regions of the electromagnetic spectrum, since it is concerned with, among other things, the indirect observation of energy levels of atoms, molecules, and nuclei. But the energy changes which give rise to microwave spectra are of a much smaller magnitude than those which cause spectra at infrared or optical frequencies. These smaller energy changes at the lower frequencies are a result of the fundamental quantum condition, $E_1 - E_2 = h\nu$ or $\nu = \frac{E_1 - E_2}{h}$, where ν is the frequency of the radiation which is emitted or absorbed, E_1 and E_2 are the initial and final energy levels of the molecules, atoms, or nuclei involved, and h is Planck's constant.

The energy level of a molecule or an atom corresponds to a particular orientation and motion of the atomic and subatomic particles. If a transition occurs in which the final energy level of the molecule or atom is greater than the initial energy level, the molecule or atom has absorbed energy from the incident electromagnetic field and the process is appropriately called

absorption. When a transition takes place in the opposite direction between energy levels, when E_1 is greater than E_2 in the fundamental equation, the process supplies energy and is called emission. Since the quantum-mechanical selection rules "allow" only certain energy transitions, the absorbed energy from a source is the energy associated with an allowed transition. If only a certain given transition takes place, the energy absorbed is ideally only the energy of one frequency, a resonant frequency or line-center frequency. Thus, energy of a given frequency is absorbed by those molecular systems with energy levels separated by the amount given by the quantum condition above, only if the selection rules allow such transitions.

Spectroscopic investigations are, hence, concerned with the measurement and explanation of the frequencies of the absorbed or emitted radiation, the widths of the spectral lines, and the spectral line intensities. These measurements require closely controlled measuring conditions because of the number of variables involved. Since the spectroscopic effects observed at microwave frequencies are very delicate ones, considerable sensitivity is required of the microwave spectrometer.

Microwave absorption spectra result from the excitation of molecules from the lower energy states to higher energy states by the incident microwave energy. The probability for a transition from a lower energy level to a higher one is exactly equal to the probability for a transition from the higher level to the lower level. If the energy in the incident electromagnetic

field is below the saturation value for the system, the observed absorption effect must then logically be a result of the difference in molecular populations between the two energy levels being considered. If P_t represents the probability of an absorption or emission transition per unit time, N_g represents the number of molecules in the ground state or lowest energy level, and N_e is the number of molecules in the excited state or higher energy level, then the probability for such a transition is given by definition as[22] $P_t = \frac{dN_e/dt}{(N_g - N_e)}$ or $P_t = \frac{dN_g/dt}{(N_e - N_g)}$. Rearranging this relationship yields $\frac{dN_e}{dt} = (N_g - N_e)P_t = -\frac{dN_g}{dt}$, and it is evident that a net absorption process requires a larger number of molecules in the ground state than in the excited state. However, if the absorption process, with its transitions from ground state to excited state, is allowed to continue for any length of time without replenishing the number of molecules in the ground state, the molecular populations of the ground and excited energy states soon become equal and absorption ceases. Thus, in order for the absorption process to sustain itself, some mechanism must exist in order that excited molecules may return to their ground state without emitting energy back to the incident electromagnetic fields.

In gases, collisions between molecules provide the mechanism required to maintain the excess ground-state molecular population. Collisions serve to maintain the gas in a state of thermal equilibrium and, thus, to relate the steady-state molecular populations by the Boltzmann distribution[22]

$$\frac{N_e}{N_g} = e^{-\frac{(E_e - E_g)}{kT}}$$

where E_e = energy of excited molecule

E_g = energy of ground-state molecule

k = Boltzmann's constant

T = absolute temperature

e = base of natural logarithms.

Since E_e is always greater than E_g, it is obvious from this equation that for all finite temperatures, the ratio of molecular populations, $\frac{N_e}{N_g}$, is less than unity; hence, N_g is greater than N_e.

The derivations thus far have assumed well-defined energy levels, each having an exact value. If such were actually the case, spectral lines would exist at only one frequency and would possess no width. But, it is an experimental fact that every known spectral line has a definite and finite width. The explanation for this finite line width, which is consistent with the energy level model of the molecule, is that there exists a certain amount of uncertainty associated with each actual energy level.

The spectral lines in the microwave region of the spectrum have essentially five different sources of line width and line broadening. These basic sources of width and broadening are as follows:[16a]

(1) Natural line width
(2) Pressure broadening
(3) Doppler broadening
(4) Wall-collision broadening
(5) Power saturation broadening.

Width and broadening sources have a cumulative effect on the line width and must be considered individually by the spectroscopist to determine the extent of the effect of each source.

Heisenberg's Uncertainty Principle indicates that the uncertainty of a given energy level of a given molecule can be expressed by δE where

$$\delta E = \frac{h}{\text{mean lifetime of the energy level in the given molecule}} . \qquad 20a$$

Thus, if the uncertainty, δE, associated with a certain level is small when compared with the amount of energy absorbed by the molecule in the transition between two energy states, the spectral line will be narrow; i.e., the range of frequencies over which absorption is observed will be small. Factors such as collisions, thermal vibration, and electric or magnetic field interactions between the atoms and molecules may cause the uncertainty of energy levels to be of considerable magnitude.

The natural width of a spectral line is due to the finite lifetime of a given energy level within a molecule. Spontaneous transitions between energy levels result in the emission or absorption of energy which is not monochromatic. It is evident from the uncertainty principle that the uncertainty of a particular energy level of a molecule is inversely proportional to the mean lifetime of that level. Thus, the natural width of a line is also inversely proportional to the mean lifetime of the energy level of interest. The natural "line width"* in cycles per second is given by the

* It is customary to measure the width of a spectral line by determining two points on the absorption curve located at half of the maximum intensity of the line and then by taking half of the frequency-width measured between these half-intensity points. This line width is symbolized by $\Delta\nu$ and has units of cycles per second or wave numbers (cm^{-1}).

theoretical equation[28a]

$$\Delta\nu = \frac{32\pi^3\nu_o^3}{3hc^3}|\mu_{m\cdot n}|^2$$

where ν_o = the resonant frequency in cycles per second

h = Planck's constant

c = speed of light

$\mu_{m\cdot n}$ = dipole matrix element.

The natural line width is not a function of the type or size of the spectrometer and is usually negligible compared with the other broadening effects found in the microwave region.

In gases, the mean lifetime of a given molecular energy level decreases as the frequency of collisions between molecules increases, thereby causing increases in δE. Since the frequency of collisions between molecules is directly proportional to the pressure of the gas for constant temperature, the line width ($\Delta\nu$) associated with the uncertainty of energy levels (δE) increases as the pressure of the gas increases. The broadening of a spectral line due to an increase in pressure is referred to as pressure broadening and is a very important part of spectroscopic measurements.

Many theories, using both quantum-mechanical and classical molecular models, have been proposed to mathematically describe the molecular interactions causing pressure broadening.[1, 15, 17, 30, 31] If the assumption is made that the duration of a molecular collision is much shorter than the mean time between molecular collisions, the classical and quantum-mechanical

models yield basically the same result. This assumption would, of course, be accurate for a small range of very low pressures only.

The distribution of molecular energies after collisions was assumed to be random by Lorentz.[15] Later, Van Vleck and Weisskopf[31] considered the energies to be related by the Boltzmann distribution. The Van Vleck-Weisskopf equations have been found to more nearly describe microwave spectra, and this theory has been almost universally accepted.

The Van Vleck-Weisskopf theory of pressure broadening assumes that intermolecular collisions constitute a random interruption of the phase of a molecular harmonic oscillator such that, after collision, each molecule assumes an independent phase. The energies of the assembly of molecules are thus distributed by the Boltzmann distribution in a state of thermal equilibrium with the incident electromagnetic fields. The expression for the attenuation due to absorption lines in gases as derived by Van Vleck and Weisskopf is

$$\gamma = 10^6 (\log_{10} e) \left(\frac{8\pi^3 \nu N}{3hc}\right) \frac{\sum_{i,j} \left\{ |\mu_{ij}|^2 f(\nu_{ij}, \nu) \right\} e^{-\frac{E_j}{kT}}}{\sum_j e^{-\frac{E_j}{kT}}} \qquad 29b$$

where γ = absorption coefficient in decibels per kilometer

ν = frequency of incident electromagnetic energy

N = number of molecules per cubic centimeter

h = Planck's constant

c = speed of light

$|\mu_{ij}|^2$ = square of the dipole matrix element connecting the states i and j

E_i, E_j = energy of the i and j states, respectively

k = Boltzmann's constant

T = absolute temperature of the gas

e = base of natural logarithms = 2.718. . .

ν_{ij} = the center frequency of the transition

$f(\nu_{ij}, \nu)$ = "structure factor" or line-shape function

$$f(\nu_{ij}, \nu) = \frac{\nu}{\pi \nu_{ij}} \left[\frac{\Delta\nu}{(\nu_{ij} - \nu)^2 + (\Delta\nu)^2} + \frac{\Delta\nu}{(\nu_{ij} + \nu)^2 + (\Delta\nu)^2} \right].$$

At frequencies near resonance, this expression yields a half-intensity half-width of $\Delta\nu = \frac{1}{2\pi\tau}$ where τ is the mean time between molecular collisions. Since the pressure is inversely proportional to the mean time between collisions, the line width due to pressure broadening is predicted to be directly proportional to the pressure of the gas.

The theory also assumes that the period of oscillation of the incident electromagnetic energy is much longer than the mean duration of a molecular collision. In the microwave region, this condition is approximated but the approximation becomes worse as the frequency of the incident electromagnetic energy is increased; such that, in the optical region of the electromagnetic spectrum, the condition is reversed and the assumption is invalid.

A knowledge of the variation of the line width with pressure is basic to the use of the Van Vleck-Weisskopf equation for predicting the intensity of absorption as a function of pressure and frequency. Since $\Delta\nu$ has been shown experimentally to be approximately a linear function of pressure over a wide range of pressures, the slope parameter, $\frac{\Delta\nu}{P}$, is an extremely useful constant of the gas and energy transition. Theoretical calculations are often not adequate to determine this parameter with the amount of precision desired; hence, it must be treated as a semi-empirical parameter. Much information on the atomic constants of molecules has been obtained by experimentation designed to measure this parameter.

Doppler broadening arises from the motion of the gas molecules which are absorbing the energy relative to the electromagnetic radiation which they are absorbing. Assuming a Maxwellian velocity distribution of the molecules, the line width is found to be

$$\Delta\nu = \frac{\nu_o}{c}\sqrt{2kN_o \ell n2}\sqrt{\frac{T}{M}} \qquad 5a, 28b$$

where T = temperature of the gas in degrees Kelvin

k = Boltzmann's constant

N_o = Avogadro's number

M = molecular weight of the gas.

It is obvious from this expression that the only simple method by which the Doppler broadening contribution to the overall width of an observed line can be reduced is by lowering the temperature of the gas.

Wall-collision broadening is due to collisions of the molecules contained within the absorption cell with the walls of the cell. Collisions between the molecules and the walls produce essentially the same broadening effect as collisions between molecules alone. When the pressure of the gas is reduced to the point where the mean free path of the molecules is roughly equivalent to the dimensions of the absorption cell, wall-collision broadening makes a significant contribution to the overall line width. The line width due to wall-collision effects is given by

$$\Delta\nu = \frac{S}{V}\left(\frac{RT}{8\pi^3 M}\right)^{\frac{1}{2}} \qquad 28c$$

where $\frac{S}{V}$ = ratio of the surface area of the absorption cell to the enclosed volume

R = the gas constant

T = temperature of the gas in degrees absolute

M = molecular weight of the gas.

Thus, wall-collision broadening can be reduced by lowering the gas temperature and by selecting the shape and size of the absorption cell with the intention of reducing the ratio of the surface area to the enclosed volume. Ordinarily, wall-collision broadening is quite small compared with other sources of broadening, but at very low pressures where the spectral lines are narrow, this source of broadening must be considered.

Power-saturation broadening occurs when the power in the incident radiation is sufficient to raise molecules from the ground state to the excited state at a greater rate than molecular collision relaxations can maintain the Boltzmann energy distribution. The result is a diminished peak intensity due to a reduced ground-state molecular population. The intensity of the absorption in the wings of the absorption line is reduced by an amount which is less than the reduction of the peak intensity. Thus, the peak intensity at the line-center frequency is reduced such that the points of half-intensity are separated by a larger amount than before, making the line-width parameter, $\Delta\nu$, appear larger. By using the minimum amount of microwave power that the sensitivity of the spectrometer will permit, power-saturation broadening effects are minimized. However, at very low pressures where there are fewer molecules involved in the absorption process, saturation effects must certainly be considered. A lower limit is thus placed on the range of pressures at which a line can be resolved and accurately measured.

III. THE OXYGEN MOLECULE: SPECTROSCOPIC ACTIVITY IN THE MICROWAVE REGION

An interaction between the incident electric field and the electric dipole moment of the molecule is the usual mechanism which couples energy from the electromagnetic fields to the molecule in gaseous microwave spectroscopy. However, the major gaseous constituents of a dry atmosphere,[23] nitrogen and oxygen, both possess no such electric dipole moment which is active at microwave frequencies. But the atmospheric oxygen molecule does possess a permanent magnetic moment; i.e., the oxygen molecule is paramagnetic. From Maxwell's equations, it is obvious that if microwave absorption can occur by electric coupling to the molecules, it can also occur by magnetic coupling. Since the electric polarity unit, the Debye unit, is approximately 100 times the magnitude of the magnetic unit, the Bohr magneton, molecular electric dipole moments are much larger than magnetic moments. Thus, the intensity of absorption due to magnetic coupling is much smaller than that due to electric coupling. Measurements of the resonant absorption of microwave energy by oxygen therefore, in general, require more sensitive spectrometers than those required for the measurement of absorption due to electric coupling.

The diatomic oxygen molecule possesses a permanent magnetic moment of two Bohr magnetons associated with the angular moment of the electronic spin.[16b] Since the spin of the unpaired electrons may take on three orientations with respect to the "end-over-end" rotation of the

molecule, each rotational energy level of the molecule is split into three levels called "triplets." If J denotes the total quantum number, then the transitions which can occur within these triplets are given by the selection rules $\Delta J = \pm 1$ and $\Delta K = 0$, where K is the rotational quantum number. The transitions between the $J = K + 1$ and $J = K - 1$ states and the $J = K$ state produce 25 major fine-structure spectral lines in the 5-mm wavelength region and only one line in the 2.5-mm wavelength region, corresponding to a variation of K from 1 to 25.[18] Thus, the oxygen spectrum in the microwave region arises from transitions between the fine-structure components of the rotational levels rather than between the rotational levels themselves. Non-resonant absorption[29c] occurs along with the resonant absorption, but the effect is a very minor one and will not be examined further in this investigation.

The single oxygen absorption line in the 2.5-mm region is of particular interest since the isolation of this line in frequency permits the measurement of the line shape and intensity without appreciable interference from other oxygen lines. The 2.5-mm oxygen line arises from the $J = 0 \rightarrow 1$, $K = 1$ transition and is referred to as the 1_- line in spectroscopy.

IV. STATEMENT OF THE PROBLEM

The resonant frequency of the 2.5-millimeter wavelength oxygen absorption line has been measured with high precision by several experimenters; however, there have been only a very few and much less precise measurements of the line shape, and even fewer measurements of the line intensity. The exact variation of the line shape with pressure over a wide range of pressures has only been estimated. Since the atmosphere is essentially opaque to frequencies near line-center frequency due to oxygen absorption, measurements of line shape and pressure broadening are essential to understanding and calculating the transmission of signals of these frequencies through the atmosphere.

Hence, the problem is to measure as accurately as possible with the equipment available the shape, both line width and intensity, of the oxygen spectral line in the 2.5-mm wavelength region over a range of pressures from a fraction of a millimeter of mercury to the atmospheric pressure of sea level. The measurements are to ascertain the absorption due to dry oxygen alone, with provisions for extrapolating the data to fit atmospheric absorption due to a mixture of dry atmospheric gases. The data should also be of sufficient accuracy to verify or refute the Van Vleck-Weisskopf equations.

V. INSTRUMENTATION

A. Elements of a Microwave Spectrometer

The microwave spectrometer differs from the optical spectroscope in the use of monochromatic or near-monochromatic sources of radiation and the corresponding absence of a dispersive element, but the same general function is performed by both instruments. Techniques for varying the frequency of microwave sources and the high precision of frequency-measuring equipment available make microwave spectroscopic measurements extremely precise ones, and, at the same time, make the instrumentation somewhat more complicated.

In its simplest form, the microwave spectrometer consists of the following components:[11a]

(1) A source of radiant microwave energy
(2) An absorption cell
(3) A device for measuring either wavelength or frequency
(4) A detector of microwave power
(5) An amplifier of the detected power
(6) An indicator.

The exact design of the various components depends upon the nature and extent of the investigation.

B. Types of Microwave Spectrometers

The first spectrometers were hybrid instruments which combined both optical and electronic methods, relying heavily on optical techniques. In 1934, Cleeton and Williams used a split-anode magnetron as a source and a rubberized cloth bag as an absorption cell.[8] Parabolic mirrors were used to direct the output of the oscillator on a grating which was used to determine the frequency. The container was filled with ammonia at a pressure slightly greater than atmospheric pressure and the intensity of the transmitted signal was measured by a thermoelectric element connected to a sensitive galvanometer. The influence of optical methods upon this spectrometer is obvious.

Since World War II, klystrons have universally replaced magnetrons as the source of electromagnetic energy for spectroscopic purposes due to the fact that klystrons are more nearly monochromatic sources. The magnetron is also more difficult to frequency modulate than is the klystron, and the higher power available from magnetrons cannot usually be utilized due to problems associated with power-saturation broadening.

In measuring the line shape over a wide range of pressures, it is necessary to take both fixed-frequency (static) and swept-frequency (dynamic) measurements. At low pressures, usually below ten millimeters of mercury, the swept-frequency method is used since the line is very narrow and the frequency of the klystron source can be swept conveniently

over a range of frequencies which is wide enough to enclose the entire width of the line. As the line becomes wider at higher pressures, fixed-frequency measurements of attenuation must be taken, while the pressure of the gas enclosed in the absorption cell is varied. The technique used in taking these measurements is to first evacuate the absorption cell and then to measure the change in absorption as the gas pressure is increased. Some microwave spectrometers cannot be used for taking both fixed-frequency and swept-frequency data without excessive modifications; however, provisions for taking both types of measurements are essential to any spectrometer designed to measure pressure broadening.

The spectrometers in common use by researchers may be classified in several different ways, but perhaps the most obvious differences between the various instruments lie in the methods of modulating and detecting the radiated microwave power. Methods of modulation include amplitude modulation, Stark modulation, source modulation, and Zeeman modulation. Although some of these modulation methods require specialized detection schemes, crystal video and superheterodyne detection systems merit some comment in a discussion of microwave spectrometers.

The simplest spectrometer is one employing amplitude modulation and crystal video detection. Although this type of system is plagued by low-frequency crystal noise and low sensitivity, improvements such as a narrow passband amplifier and a data-sampling system synchronized to the frequency of the amplitude modulation[21, 24] make the system a very

practical one for use at frequencies where enough transmitted power is available to permit the use of a less sensitive detection system.

In an attempt to improve the signal-to-noise ratio and to increase sensitivity, three methods of modulation -- source modulation, Stark modulation, and Zeeman modulation -- were devised.

The term "source modulation" is usually used to refer to a technique designed to overcome low-frequency crystal noise by frequency modulating the signal source at radio frequencies and by using the absorption line for detection. Since the spectral line acts as a discriminator, converting the frequency modulated signal into a signal of varying amplitude, a simple AM radio receiver can be used to amplify the received signal. When the system is adjusted properly, the receiver detects the first derivative or the slope of the absorption curve. The source modulation system using the absorption line for detection represents somewhat of an improvement in sensitivity over the crystal video system, but the sensitivity is appreciably reduced when operating at the wing frequencies of a line where the received power is not very frequency-dependent. Another disadvantage of the source-modulated, line-detected, spectrometer is that any frequency-dependent power change will be detected, including changes in the standing wave ratio of the system.

Stark modulation was introduced as a method of increasing the sensitivity of spectrometers. The absorption frequencies of polar molecules are shifted in the presence of an electric field due to the Stark

effect. Stark modulation involves the application of a radio-frequency voltage to an electrode which runs the length of the absorption cell and the use of a radio receiver placed after the crystal detector and tuned to the modulating frequency. The crystal and tube noise as well as noise due to klystron power variations are reduced by this molecular modulation scheme. Disadvantages of Stark modulation include the obvious inability of the system to function when gases such as oxygen, which possess no electric dipole moment, are investigated; the critical placement of the electrode within the absorption cell; and the difficulty of obtaining a uniform electric field.

The magnetic modulation analog of Stark modulation is called Zeeman modulation and may be used for investigations of paramagnetic molecules such as oxygen. The Zeeman absorption cell is difficult to construct since a high-frequency uniform magnetic field must be applied to the gas. Problems involving eddy currents within the cell and interactions with stray magnetic fields make the Zeeman spectrometer difficult to use for the measurement of the delicate paramagnetic resonance effects. The Zeeman modulation system facilitates the investigation of the Zeeman effect in molecules, but leaves much to be desired as a modulation device for a microwave spectrometer.

C. The Design of a Spectrometer for this Investigation

For the investigation of the oxygen line at 118.75 Gc, a 500-foot long, six-inch diameter, outer copper conductor of a coaxial line

was used as the absorption cell. The cell, shown in Figure 2, has two glass-supported teflon dielectric "windows," one at each end, and is equipped with two vacuum pumps, several primary pressure gauges, and provisions for injecting gas. Two 10' by 20' equipment buildings, one located on each end of the cell, were also available.

The cell was found to be ideal for the purposes of this investigation for the following reasons:

(1) The enclosed volume is sufficient to prevent wall collisions at the lowest pressures

(2) The diameter is large enough in terms of wavelengths to permit propagation approaching free-space propagation

(3) The length is sufficient to permit the absorption of a measureable amount of energy by the enclosed gas.

The design of the associated instrumentation was approached with the object of optimizing the use of the available cell.

Designing and building a waveguide transition that would match the small waveguide to the six-inch diameter cell without the propagation of undesirable modes through the cell is impractical. Transmission through the cell was accomplished by propagating a wave from a conical horn antenna such that it was incident upon the dielectric window essentially as a plane wave. Reflections from the teflon windows were eliminated by making the windows an exact multiple of a half-wavelength thick. Propagating a plane wave necessitates the location of the antennas at a distance far

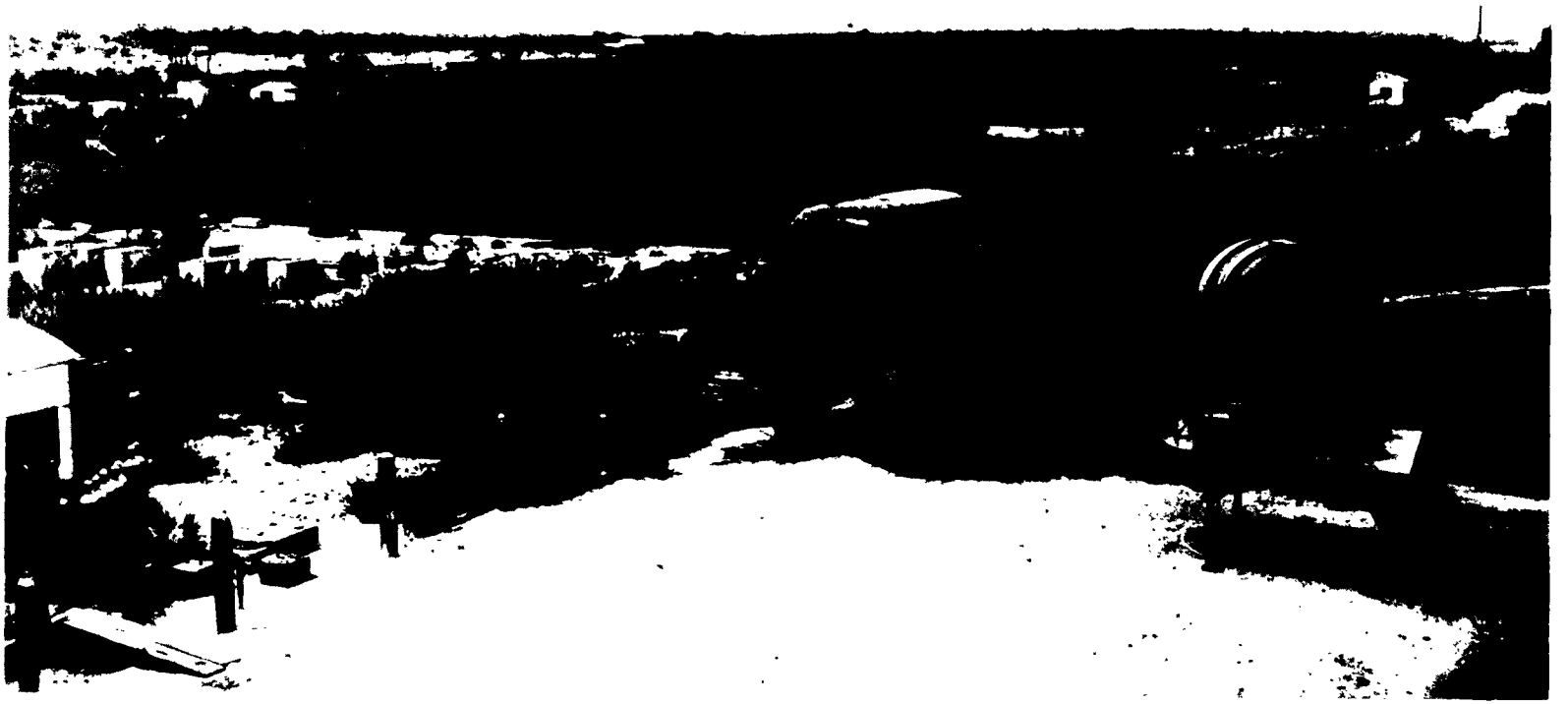

THE 500-FOOT LONG, 6-INCH DIAMETER,
ABSORPTION CELL
FIG. 2.

enough away from the cell in order that there is a maximum of $\frac{\lambda}{8}$ variation in path length over the three-inch radius of the cell. Calculations for this condition are shown in the appendix. By reciprocity, the length of the transmitting antenna from the cell and the length of the receiving antenna from the cell should be equal.

There are two basically similar methods for generating coherent radiation of these frequencies both of which are available and satisfactory for use in this investigation.

A klystron operating in the 56 to 65 Gc range may be used as a primary signal source with a non-linear device placed in the waveguide to generate the second harmonic output power. If the non-linear device is followed by a very small section of waveguide, the fundamental frequency will be below cut-off for the smaller waveguide and only the higher harmonic components will be transmitted. The standard non-linear device for harmonic generation is a germanium or silicon crystal. By the use of crystal harmonic generators, frequencies in the higher frequency regions of the spectrum can be produced with less expensive klystrons. However, greater demands for regulation are placed upon the klystron power supply to achieve the desired monochromatic radiation.

The alternative available method for achieving output at these frequencies is a newly-developed imported reflex klystron with a fundamental frequency output from 108 to 122 Gc. At the present time, the merits of this klystron have not been proven sufficiently to justify the higher purchase

price, even though the power output is significantly greater than that obtained by using crystal harmonic generators with the 60-Gc klystrons. Other disadvantages of this klystron include critical current regulatory circuits; e.g., the filament current must be maintained at exactly 1.80 $\pm$ 0.01 amperes. Thus, the 57 to 62 Gc klystron with crystal harmonic generator was chosen as the radiation source.

The power lost in free-space coupling the transmitting and receiving antennas to the absorption cell, together with the relatively low level of 118 Gc signal from the crystal harmonic generator, requires the use of heterodyne detection techniques. The sensitivity required of the detector precludes the use of a simple video detection system.

The length of the absorption cell makes Zeeman modulation impractical due to the problems associated with producing the necessary uniform magnetic field. The Stark modulation system cannot be used to measure the oxygen resonances, and source modulation with absorption line detection is impractical due to the failure of the source-modulated, line-detected, spectrometer to function efficiently under fixed-frequency operation in the wings of the line.

A system with the transmitter frequency-modulated at an audio frequency and a superheterodyne receiver with a local oscillator which is frequency modulated at a higher audio frequency possesses the qualitites desired for this spectrometer. For swept-frequency measurements, provision must be allowed for frequency modulating the transmitter, while for

fixed-frequency measurements, the transmitter must be held at a known constant frequency.

The reflex klystron is extremely easy to frequency modulate. The frequency of oscillation is approximately a linear function of the reflector voltage over a small range of voltages. Although the power output is also a function of the reflector voltage for a fixed klystron cavity position, the variation of power over a small range of reflector voltages may be made negligible by proper adjustment of the voltages and cavity dimensions. By impressing a known voltage waveform on the reflector of the klystron, the time variation of output frequency is known.

Consider the case where the frequency of the transmitter is set to a certain fixed frequency. If the local-oscillator klystron of the superheterodyne receiver is modulated with a sinusoidal voltage, then the frequency to which the receiver is tuned varies approximately sinusoidally about the unmodulated frequency of the local oscillator. If, at the receiver, a linear mixer is used to mix the local oscillator signal with the incoming signal from the transmitter and a crystal detector is used to detect the beat frequencies, then the output of the intermediate-frequency amplifier will exist only for the instants that the difference between the two frequencies is equal to a value within the bandpass of the tuned amplifier. Since the crystal detector acts as a square-law device, the output of the crystal, and hence the input to the IF amplifier,is approximately a direct linear function of the power received for large signal-to-noise ratios. The output of the IF amplifier is approximately a linear function of its input;

hence, the output of the amplifier is a measure of the power reaching the receiver. If the output of the amplifier is fed to an integrator which responds to the peak output voltage, then the output of the amplifier can be displayed as a DC current through a pen recording-milliameter. If the power from the local-oscillator klystron is essentially constant, and therefore the crystal conversion efficiency constant, the output current through the pen recorder is proportional to the power received by the receiver.

The system described above represents the best apparent use of the available equipment and is the system to be used for this investigation. Calibrated attenuators are available which allow the injection of a known amount of power loss into the system. The installation of a calibrated attenuator in the waveguide at the receiver between the incoming signal from the transmitter and the mixer permits the calibration of the pen recorder to read power changes directly in decibels. The completed system described thus far is a very precise fixed-frequency spectrometer.

But the design of a fixed-frequency spectrometer is only part of the problem. Consider now the possibility of modifying the system to be used to make swept-frequency measurements. Swept-frequency measurements require the frequency of the transmitter to be changed in a known manner such that the received signal displays the resolved line on a calibrated frequency scale. If the local oscillator klystron of the receiver is frequency modulated with a 6000 cps signal while the klystron of the transmitter is frequency modulated with a 60 cps signal synchronized to the

primary 115-volt AC power line frequency; then, if the output of the IF amplifier is displayed on an oscilloscope swept at a 60 cps rate with adjusted phase, the oscilloscope should trace the outline of the oxygen absorption curve. The system is thus a data-sampling system where the receiver samples the transmitted signal at intervals determined by the frequency of the modulating voltage of its local oscillator. For the 6000 cps and 60 cps system described above, the output of the IF amplifier would be 100 bandpasses per sweep of the oscilloscope. The x-axis would then approximate a linear frequency scale which can be calibrated by a knowledge of the bandpass of the IF amplifier.

A block diagram of the spectrometer showing the arrangement of components both for swept-frequency and fixed-frequency operation is shown in Figure 3.

The design as explained above presents no obvious practical problems; however, when the system was constructed, the following problems were observed:

(1) The line-center frequency did not appear at exactly the same position on every trace and retrace due to a "hysteresis" effect, associated with the frequency modulation of the transmitting klystron, that could not be corrected by the use of the phase-shifting network.

(2) The available oscilloscopes did not have the necessary bandwidth to respond to the frequencies in the signal from the IF amplifier.

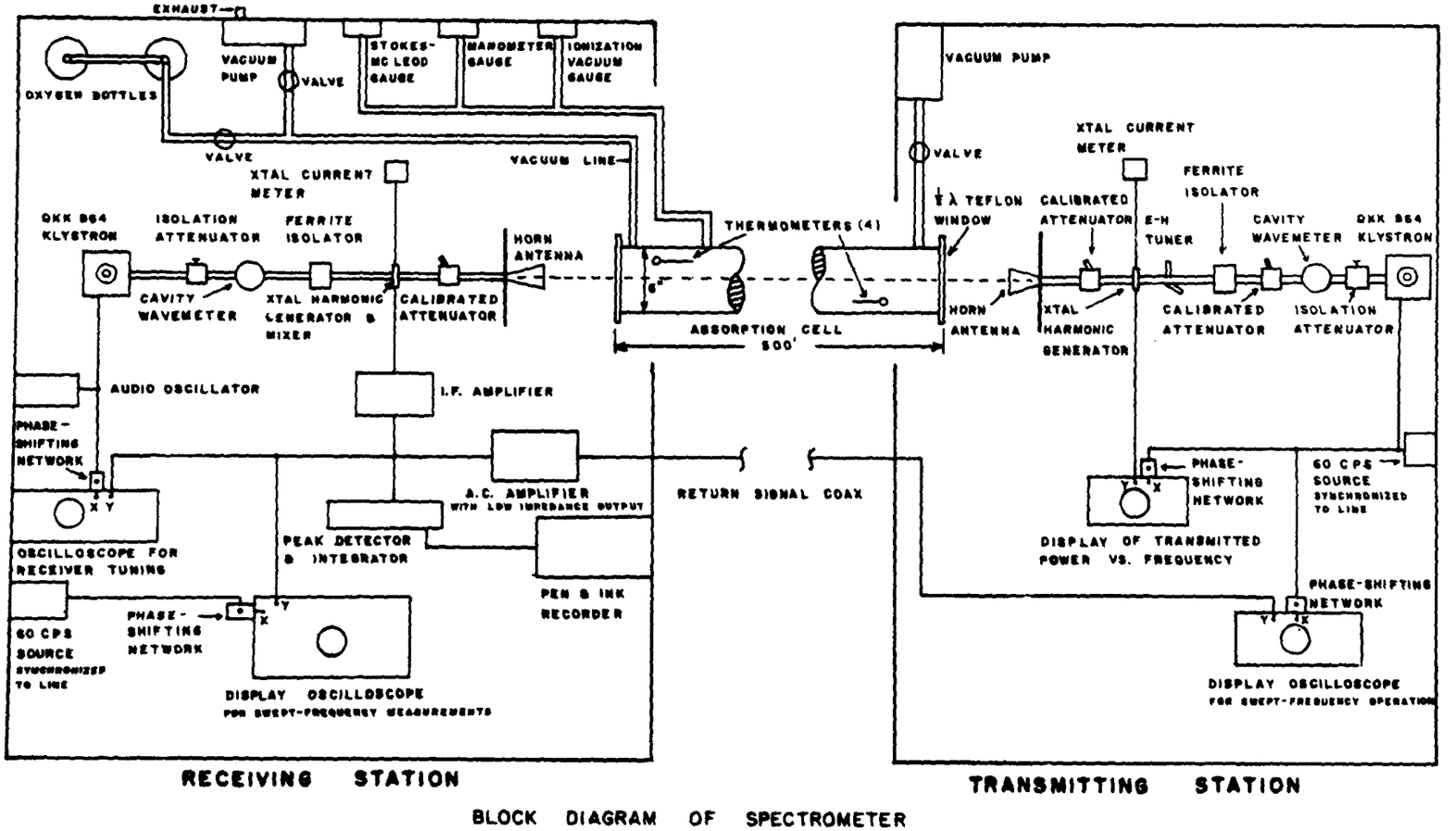

BLOCK DIAGRAM OF SPECTROMETER

FIG. 3

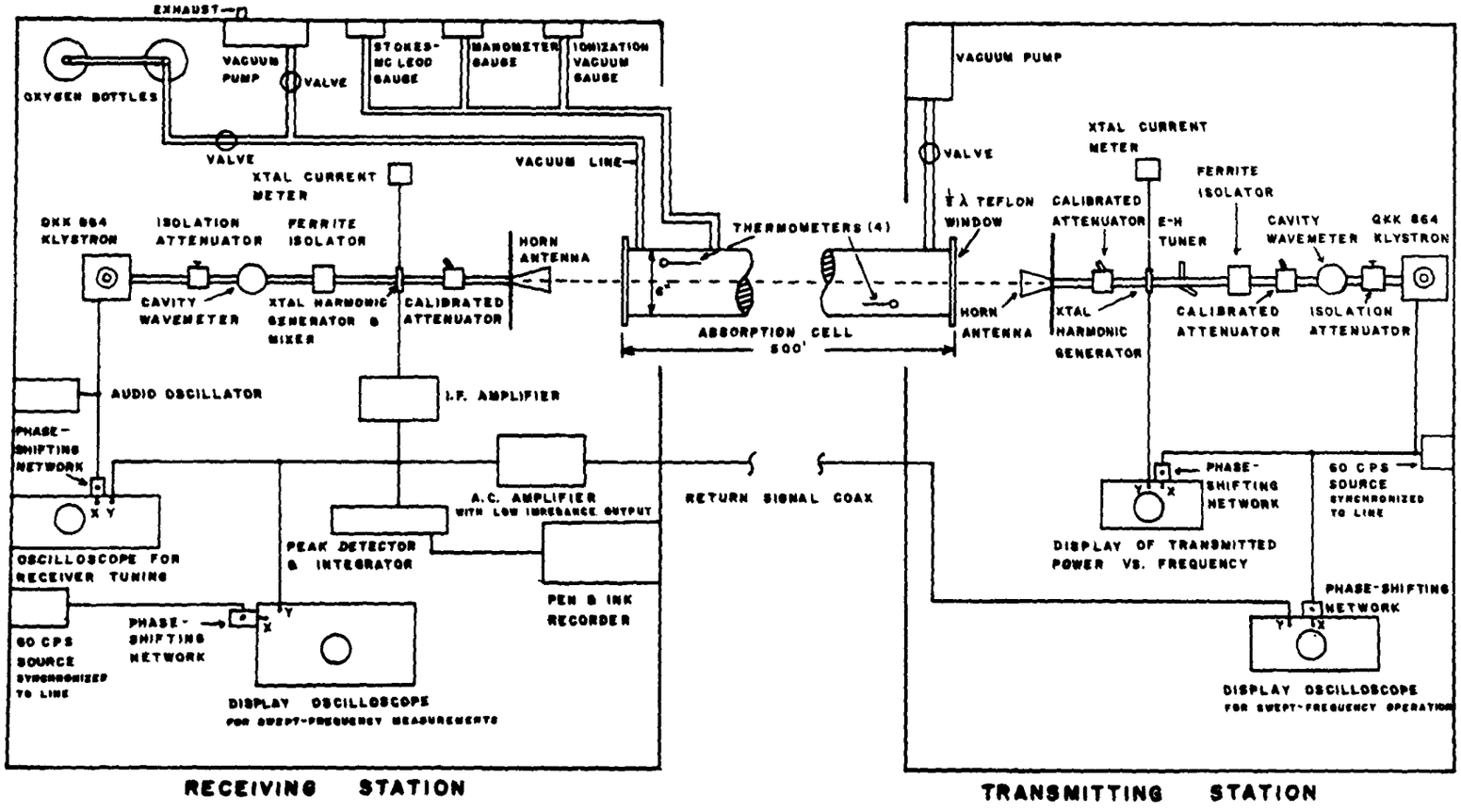

BLOCK DIAGRAM OF SPECTROMETER

FIG. 3

Hence, a compromise design was necessary. The receiver modulation frequency was changed to approximately 1000 cps without noticeably affecting the accuracy due to decreased sampling rate. The bandwidth of the two oscilloscopes was adequate to display the output of the IF amplifier for this signal. Next, the display oscilloscope was internally swept with a sawtooth waveform synchronized to the 60 cps line frequency and adjusted such that each sweep of the oscilloscope represented a sweep of the transmitting klystron frequency in the same direction. This corrected the hysteresis phenomenon, but the linear oscilloscope sweep distorted the frequency presentations on the x-axis of the oscilloscope from linear to sinusoidal. This was not a serious disadvantage, however, since a knowledge of the modulation of the transmitter permitted calibrating the display as shown in the appendix. It was thus possible to modify the theoretical system to use the available equipment while preserving the information-bearing attributes of the signal.

Photographs of the operational system are shown in Figures 4 through 7.

The Stokes-McLeod high-vacuum gauge, Miriam absolute-pressure manometer, Alphatron ionization vacuum gauge, oxygen bottles and associated cell-pressurizing equipment are shown in Figure 4.

Figure 5 shows the receiver as viewed from the receiving end of the absorption cell. Visible in Figure 5, and utilized as indicated in Figure 3, are the conical antenna, radiation absorbing shield, two Tektronix RM503

oscilloscopes, Tektronix oscilloscope camera, two phase-shifting networks, Hewlett Packard model 466A AC amplifier, Hewlett Packard audio oscillator, Texas Instruments Incorporated Recti-Riter pen and ink recorder, peak detector-integrator and IF bias supply, three Lambda DC power supplies, FXR model Z815B universal klystron power supply, klystron voltage control panel, and two Sorenson AC voltage regulators.

A close-up view of the receiver is shown in Figure 6. This photograph reveals the instrumentation hidden by the absorbing shield in Figure 5. Components visible in Figure 6 include the horn antenna, radiation absorbing shield, Demornay-Bonardi model DBW-410 calibrated attenuator, FXR crystal harmonic generator and mixer, TRG ferrite isolator, Narda model M807 cavity wavemeter, isolation attenuator, Raytheon QKK 864 klystron, L. E. L. Inc. IF amplifier, klystron cooling fan, and crystal current meter.

The transmitter, similar in many respects to the receiver, is shown in Figure 7. Visible in this photograph are the calibrated attenuator, FXR crystal harmonic generator, E-H tuner, TRG ferrite isolator, cavity wavemeter, isolation attenuator, Raytheon QKK 864 klystron, two Tektronix type 541 oscilloscopes, and portions of the absorbing shield and crystal current meter.

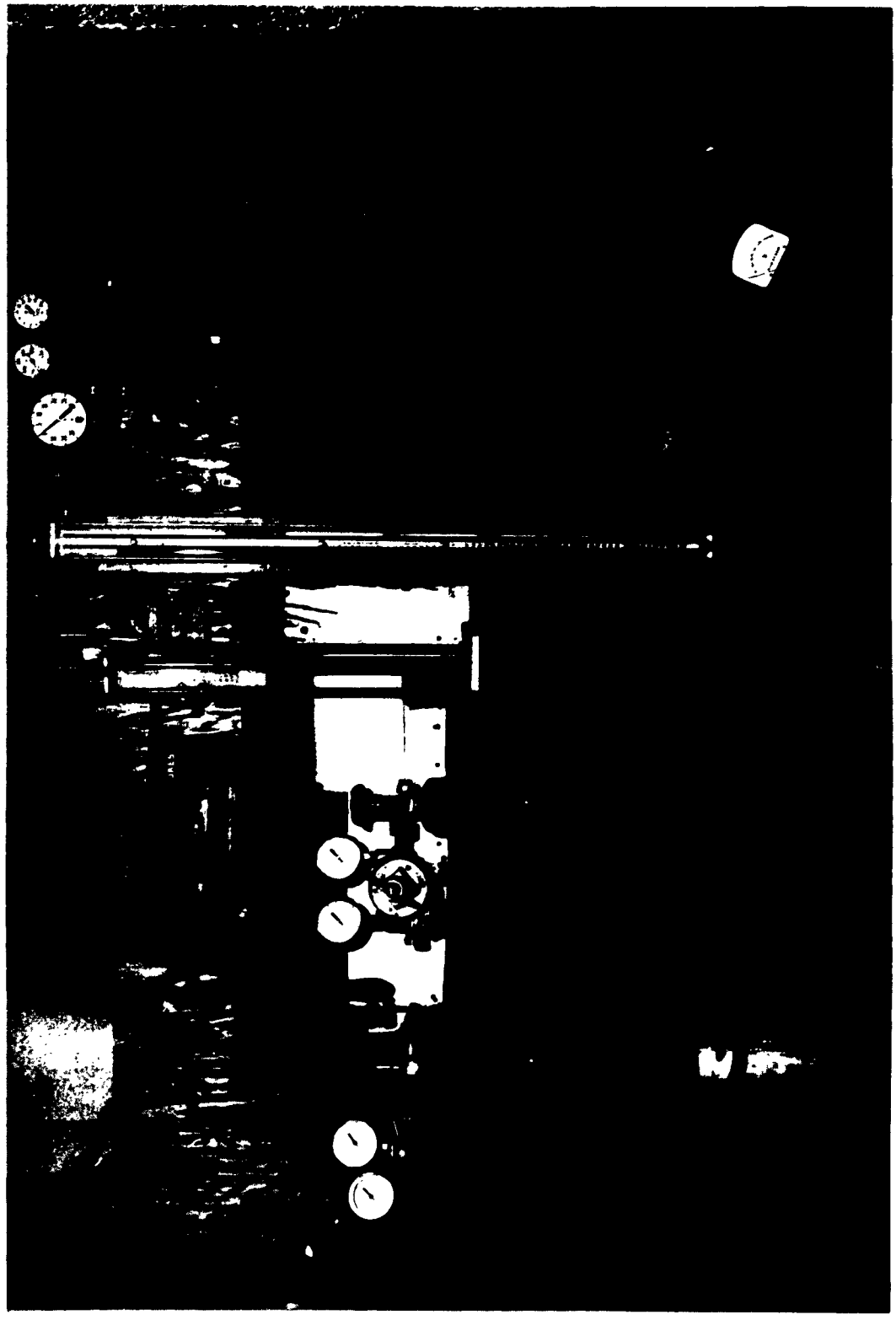

THE PRESSURE GAUGES, OXYGEN BOTTLES, AND ASSOCIATED CELL-PRESSURIZING EQUIPMENT
FIG. 4.

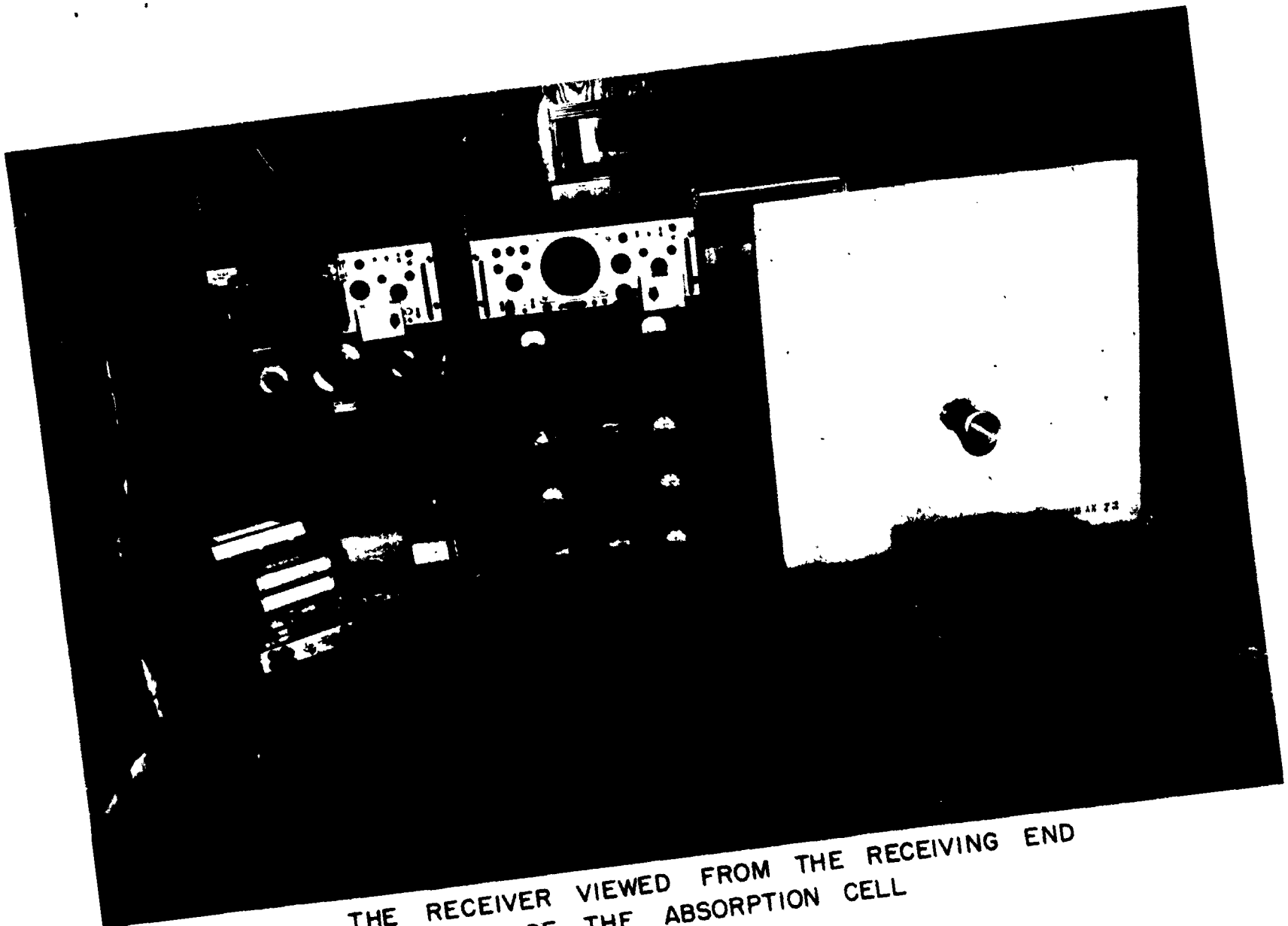

THE RECEIVER VIEWED FROM THE RECEIVING END
OF THE ABSORPTION CELL
FIG. 5.

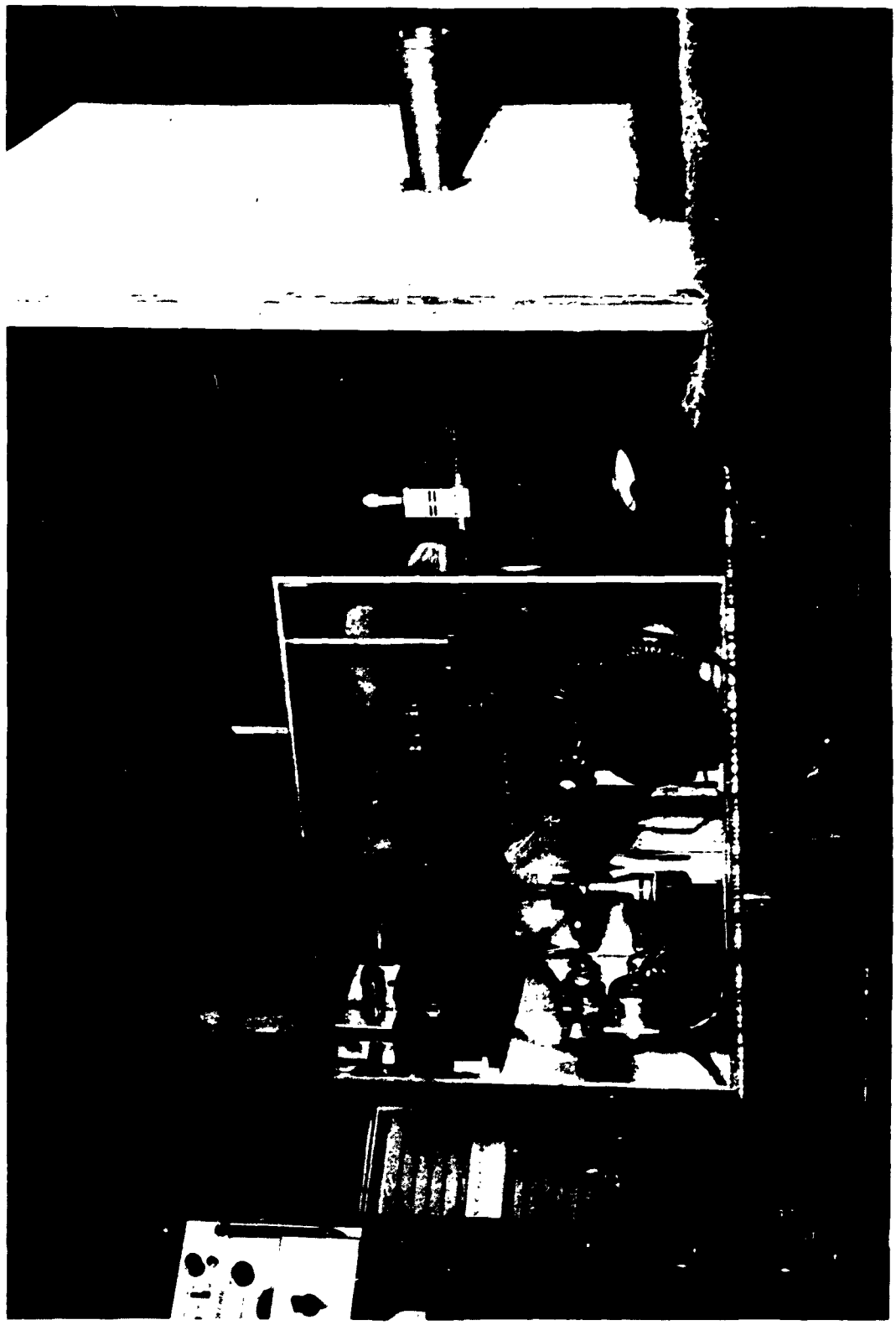

A CLOSE-UP VIEW OF THE RECEIVER
FIG. 6.

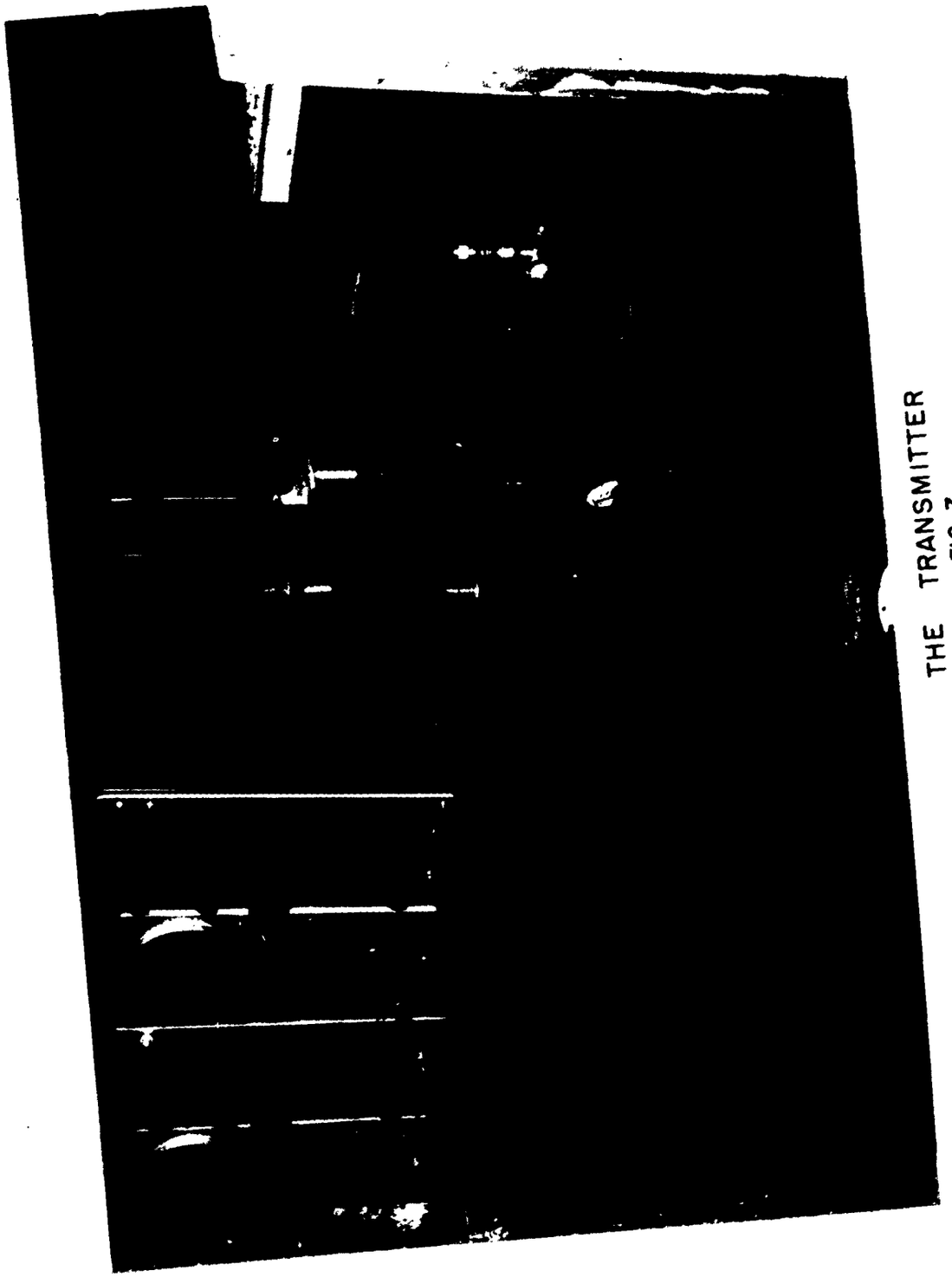

THE TRANSMITTER
FIG. 7.

VI. TECHNIQUES OF MEASUREMENT

A. Dynamic-Frequency Techniques

Dynamic-frequency measurements of the peak intensity of the absorption line and the line width at pressures of 0.5, 1.0, 1.5, 2.0, 3.0, 3.5, 4.0, 4.5, 5.0, and 6.0 millimeters of mercury were the first measurements to be taken with the spectrometer. For these measurements, the frequency of the transmitter was set as closely as possible to the line-center frequency using the cavity wavemeter. The receiver was tuned to center the transmitted signal within the frequency sweep of the local oscillator by observing the display of the receiver-tuning oscilloscope indicated in Figure 3. A 60 cps sinusoidal modulation signal was then applied to the transmitting klystron to achieve swept-frequency output.

With oxygen enclosed in the cell under an absolute pressure of approximately two millimeters of mercury, the frequencies of the transmitter and receiver were tuned, until the line was located on the display oscilloscope. The amount of tuning required to locate the line after preliminary setting of the frequency by wavemeter was usually of the order of 20 Mc or less. After the line was located, the absorption cell was evacuated to a pressure of 0.5 millimeters of mercury, the minimum pressure at which the line was of measureable magnitude. Photographs of the attenuation versus frequency data displayed on the oscilloscope were taken with an oscilloscope camera at selected pressures up to six millimeters of mercury.

Transmitter frequency sweep deviations were calibrated on the oscilloscope by measuring the passband of the IF amplifier with a frequency generator and by then photographing the bandpass when located in the center of the oscilloscope display. The received signal level was calibrated by photographing the deflection on the display oscilloscope for known amounts of calibrated attenuation injections at the receiver. A complete set of data was taken at each pressure setting, the pressure being set by the use of a Stokes-McLeod type high-vacuum gauge. The temperature of the oxygen enclosed in the absorption cell was determined with four mercurial thermometers, shielded from direct sunlight and attached to the cell with a grease of high thermal conductivity at selected locations along the cell.

B. Static-Frequency Techniques

Static-frequency measurements of oxygen attenuation at pressures of 8, 15, 30, 60, 100, 200, 300, 400, 500, 600, 700, and 760 millimeters of mercury were taken at frequencies of 30, 60, 120, 240, 480, 1000, 2000, and 4000 megacycles per second on both sides of the line-center frequency.

The 30-Mc center frequency of the narrow-band IF amplifier was utilized in precisely setting the desired transmitter frequencies between line-center and 1000 Mc on either side of line-center. The transmitter frequency was first located at line-center and then the desired frequency of the transmitter was set by relocating the IF passband appearing on the receiver-tuning oscilloscope. In this manner, multiples of 30 Mc in frequency could be precisely set. This method of setting frequency was necessary since

the Q of the cavity wavemeters was not high enough to determine the frequencies with the precision required for the measurements. At frequencies of approximately 1000 Mc or greater on either side of the line-center frequency, the frequency could be just as accurately set using the wavemeter because of the large number of repeated IF passband relocation steps required to set these frequencies.

Fixed-frequency measurements were taken by first evacuating the absorption cell to a pressure low enough to provide an unmeasurable amount of oxygen absorption at the frequency of interest; e.g., 1 mm Hg at 30 Mc from line center or 10 mm Hg at 4000 Mc from line center. The chart of a pen and ink recorder was then calibrated using the calibrated attenuator, and oxygen was injected into the cell while the attenuation as a function of pressure for the pre-set frequency was recorded. In this manner, a minimum of two complete runs were made at each frequency. The attenuation in db/500 ft at the marked pressures on the chart was determined by using a calibration curve obtained from the known attenuation steps applied to the recordings. The attenuation data were converted from db/500 ft to db/km by simply multiplying by the factor 6.56 (500 ft/km). Gas temperature was measured with the mercurial thermometers in the same manner as for the swept-frequency measurements, and pressures were set using a mercurial absolute-pressure manometer.

C. Operational Intricacies

Several intricacies were involved in operating the equipment. The phase-shifting networks on all oscilloscopes had to be set so that trace

and retrace overlapped without distorting the information contained in the signals. During swept-frequency measurements, the transmitter had to be adjusted for optimum "flat" power output across the frequency-scan using the display of the transmitted power versus frequency given by the oscilloscope located at the transmitter. The crystal current meter at the receiver had to be precisely set to a value that represented the most favorable compromise between noise generation and conversion efficiency. The audio oscillator used to sweep the frequency of the receiver had to be adjusted in order that the sweep of the local oscillator was large enough to enclose the spectrum of the transmitter, but not so large as to enclose both heterodyne frequencies. The frequency of the klystron of the receiver had to be maintained at the same value throughout the length of time required to record the data.

Since accurate data on the dielectric constant of glass-supported teflon are not known for frequencies in the 10^{11} to 10^{12} cps range, the condition that the windows be an exact multiple of one-half wavelength thick could not be reliably calculated. The windows were chosen experimentally for minimum reflections and were tested each time significant frequency changes were made.

Typical samples of oxygen absorption data of the 118.745 Gc line obtained by measurements using the absorption cell are shown in Figure 8. Figure 8(A) is typical of the swept-frequency data at a pressure of two millimeters of mercury, and Figure 8(B) is typical of the chart recording of fixed-frequency data at a frequency of 119.745 Gc.

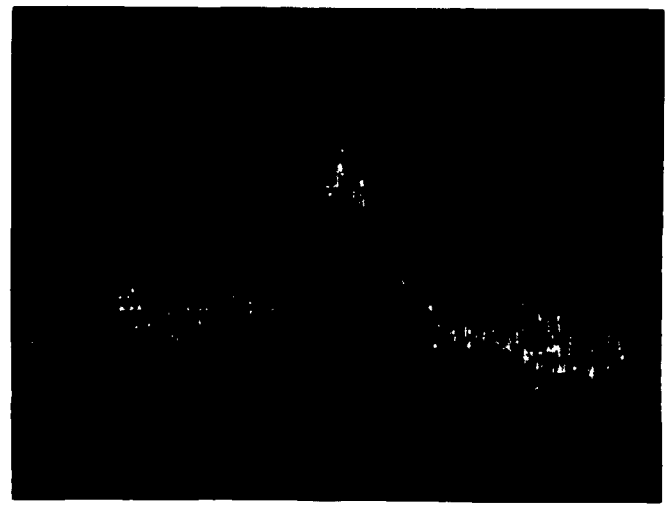

(A) TYPICAL SWEPT-FREQUENCY DATA PHOTOGRAPH

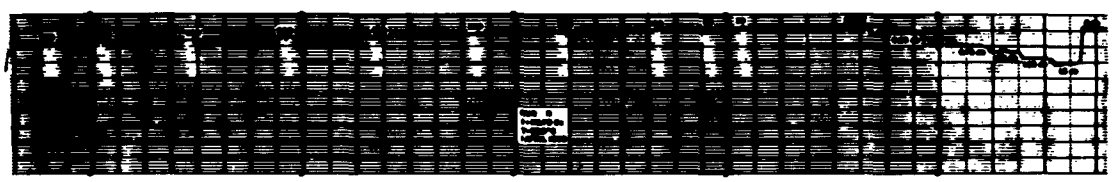

(B) TYPICAL FIXED-FREQUENCY CHART RECORDING

SAMPLES OF OXYGEN ABSORPTION DATA OBTAINED BY USE OF SPECTROMETER

FIG. 8.

VII. THE DATA

The measured values of attenuation, line width, and peak intensity for the oxygen absorption line in the 2.5-mm wavelength region of the spectrum are shown as a function of frequency and pressure in Figures 9 through 15. Calculated curves representing the "best fit" to the experimental data of the Van Vleck-Weisskopf line shape together with the experimental data used to determine the calculated curves are shown in Figures 9 through 11.

The curve of $\Delta\nu$ versus pressure shown in Figure 12 was derived using the average value of $\Delta\nu$ obtained from the calculated curves. Figure 13 shows the measured values of peak intensity versus pressure.

Figure 14 is a graph of the half-intensity, half-width versus pressure obtained by the swept-frequency technique. Also shown on this graph are the points that were calculated by the use of the peak intensity and the constants found to best describe the absorption curves at the higher pressures. The slopes obtained by swept-frequency and fixed-frequency techniques are both shown in Figure 14. In Figure 15, the measured peak intensity of the line is plotted versus pressure.

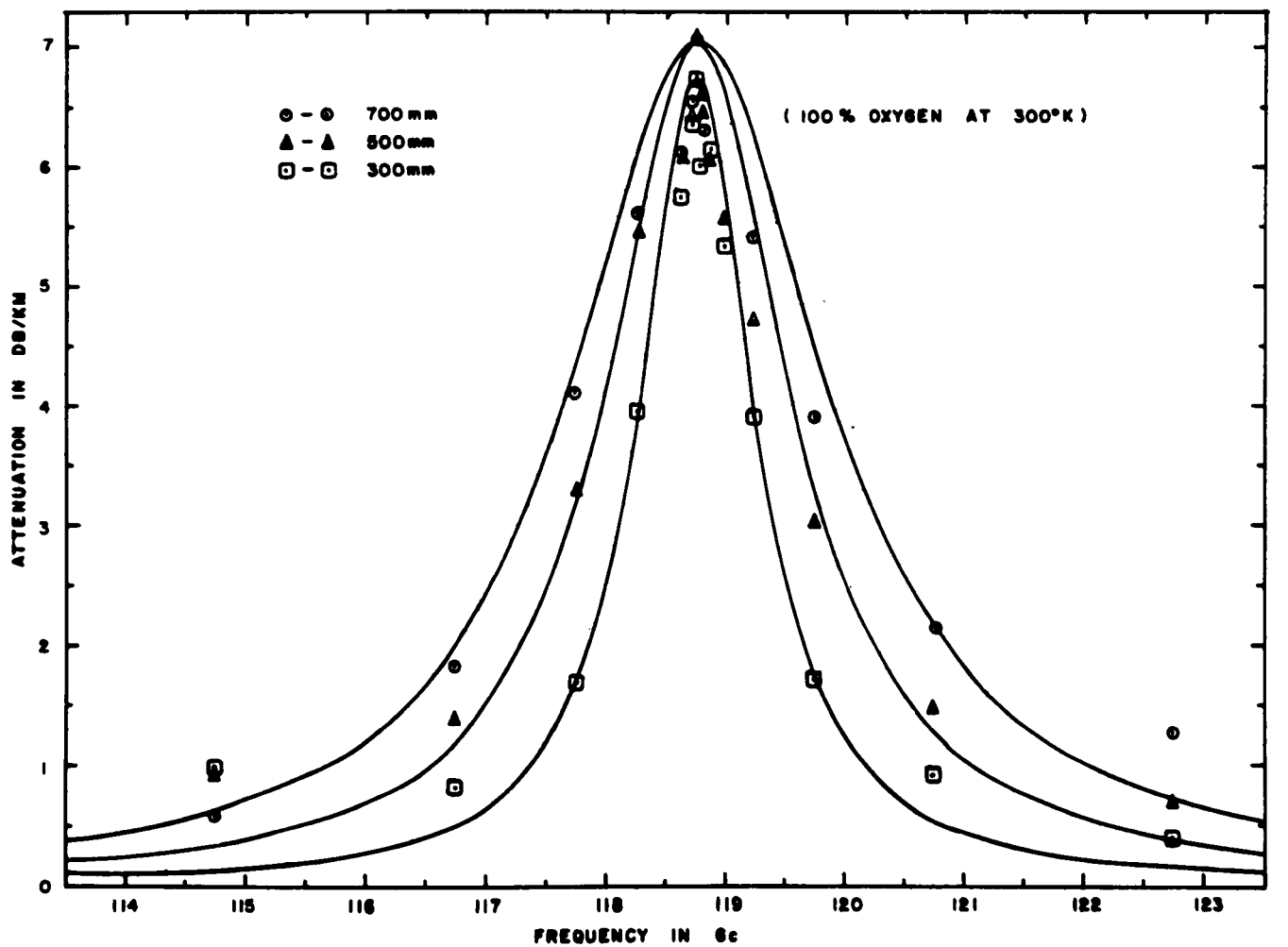

ATTENUATION VERSUS FREQUENCY FOR PRESSURES OF 700, 500, AND 300 MILLIMETERS OF MERCURY.

FIG. 9.

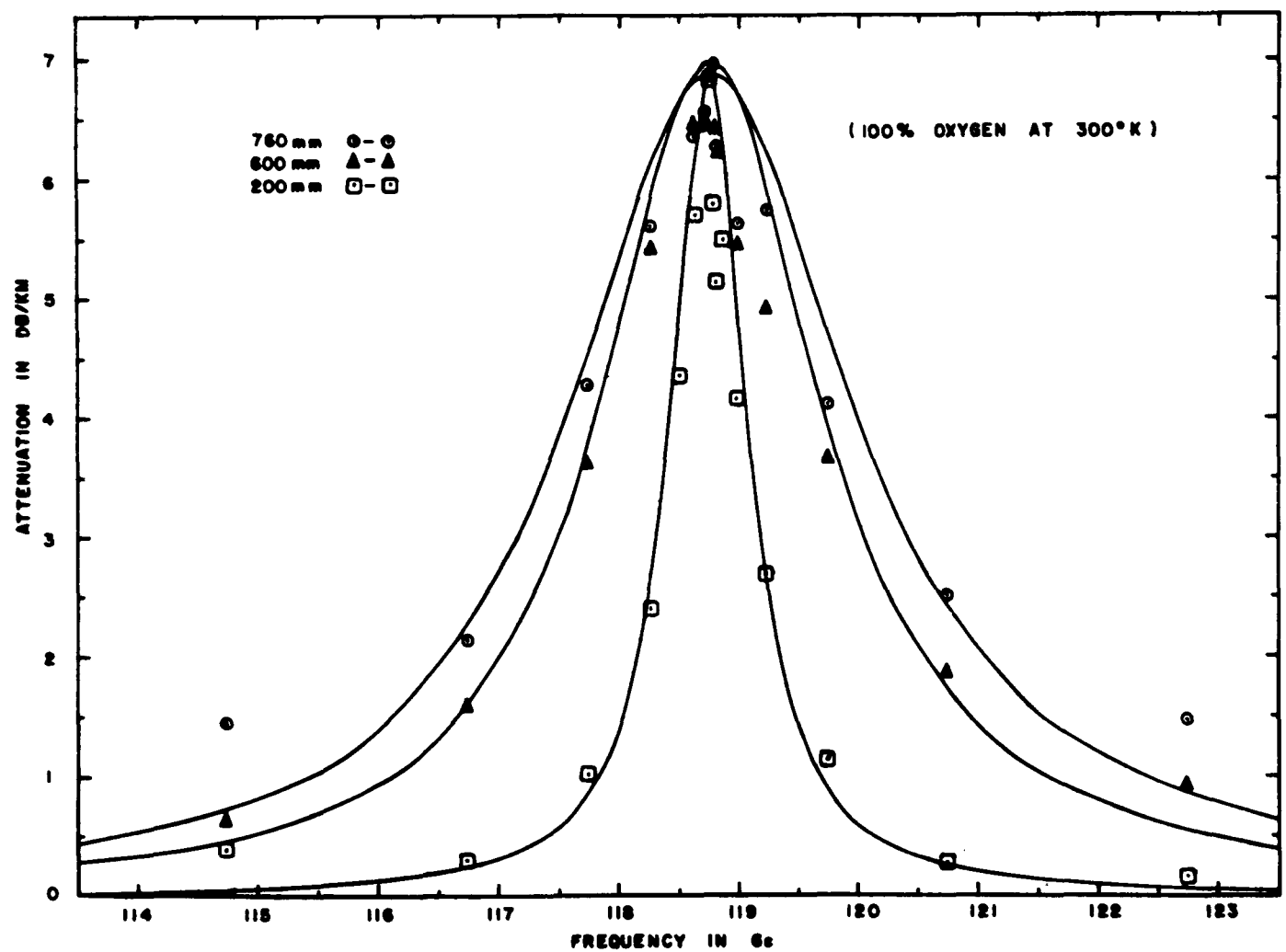

ATTENUATION VERSUS FREQUENCY FOR PRESSURES OF 760, 600, AND 200 MILLIMETERS OF MERCURY.

FIG. 10.

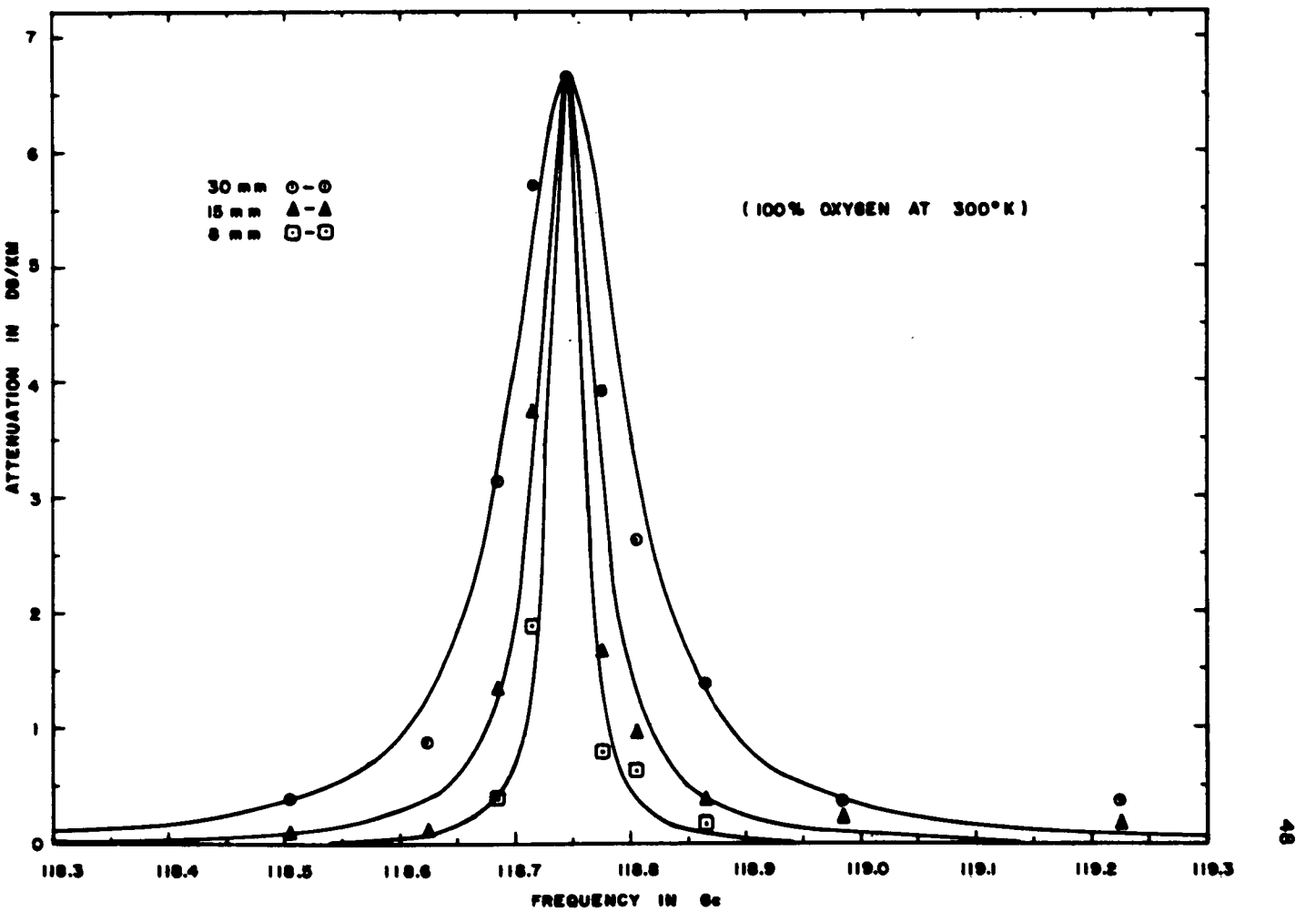

ATTENUATION VERSUS FREQUENCY FOR PRESSURES OF 30, 15, AND, 8 MILLIMETERS OF MERCURY.

FIG. 11.

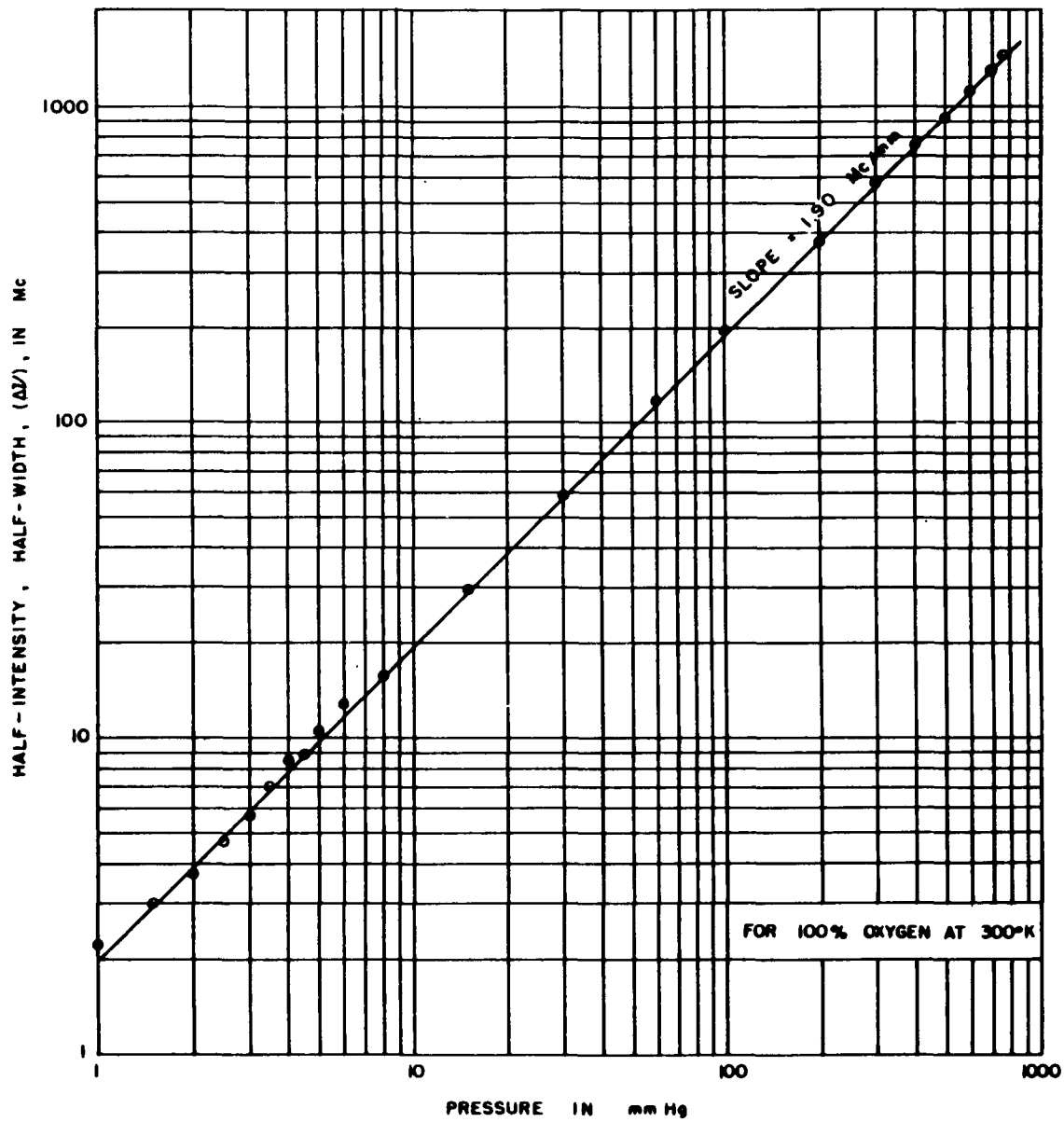

HALF-INTENSITY, HALF-WIDTH OF LINE VS. PRESSURE

FIG. 12.

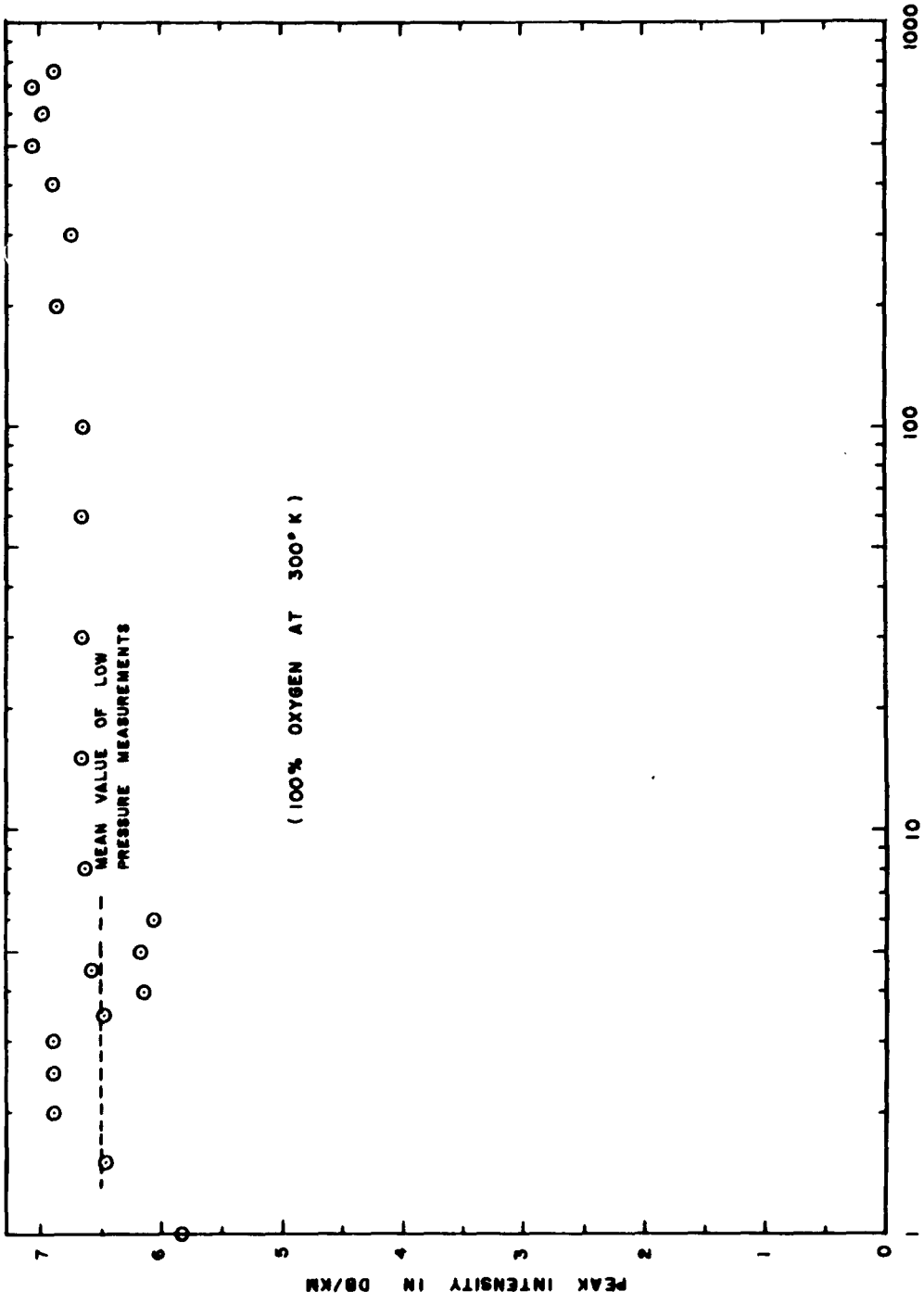

PEAK INTENSITY OF LINE VS. PRESSURE.

FIG. 13.

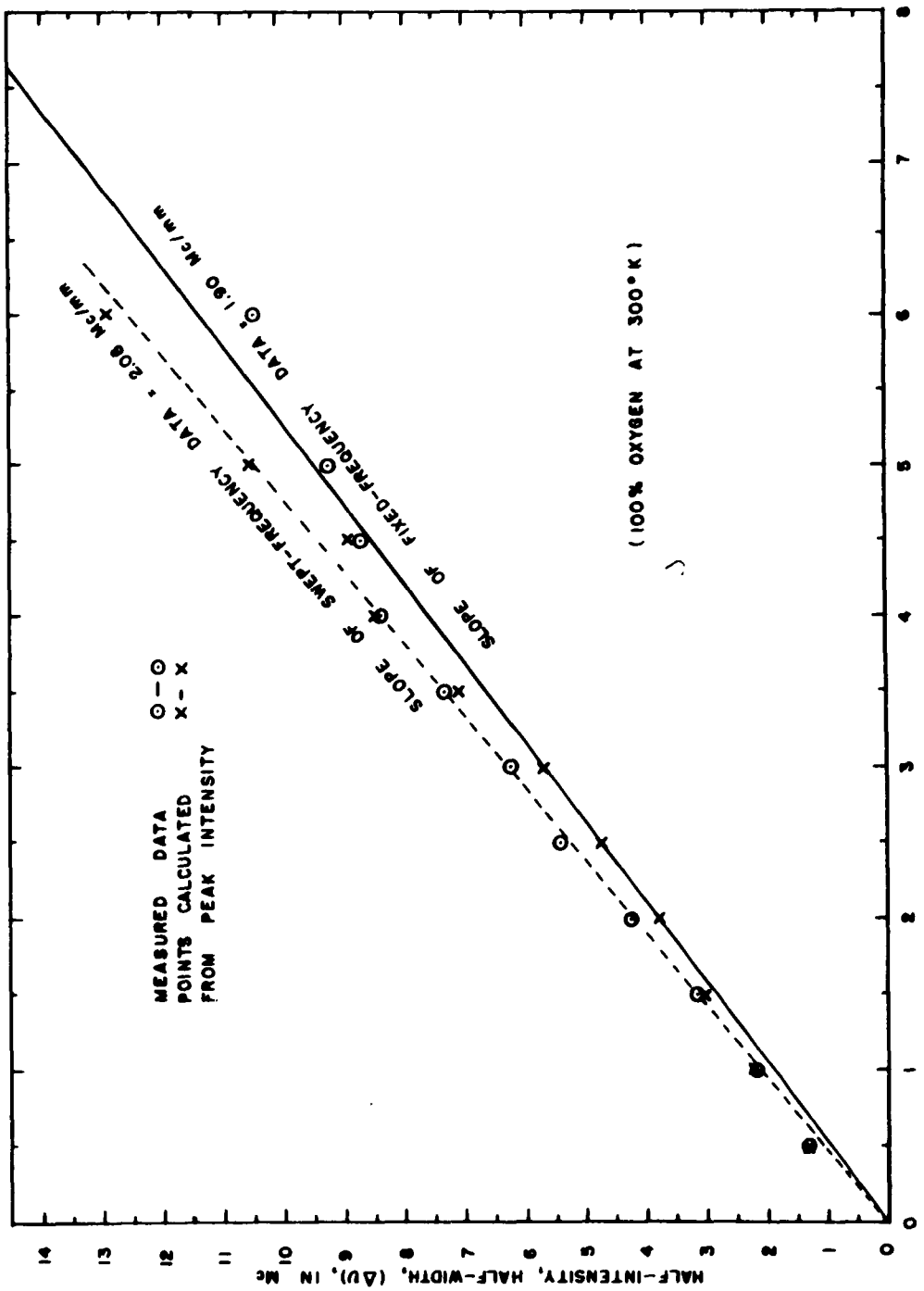

HALF-INTENSITY, HALF-WIDTH OF LINE VS. PRESSURE FOR LOW PRESSURES.

FIG. 14.

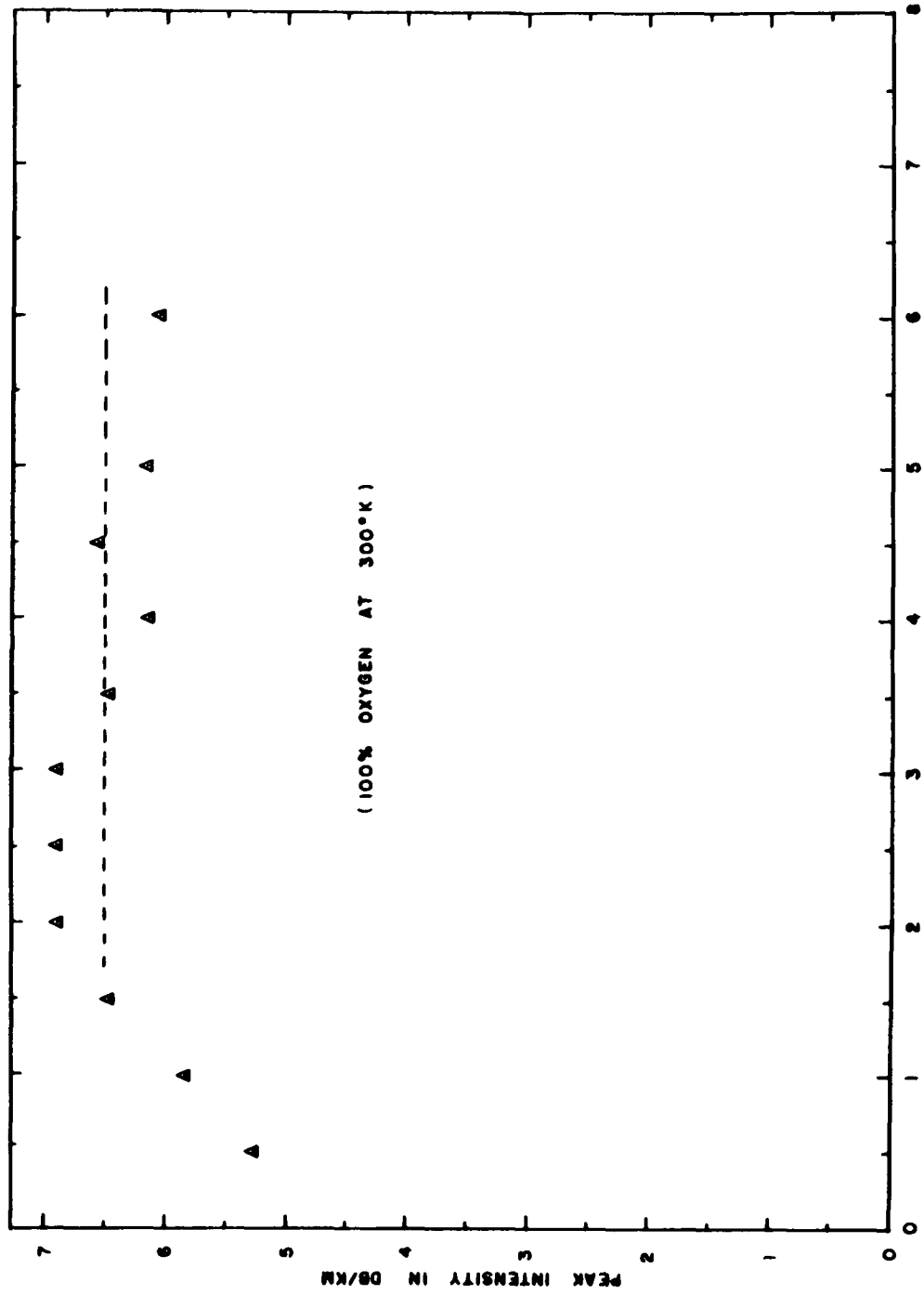

PEAK INTENSITY OF LINE VS. PRESSURE FOR LOW PRESSURES.

FIG. 15.

VIII. DISCUSSION AND ANALYSIS OF DATA

Since facilities for controlling the temperature of the absorption cell were not available, the data of this investigation were taken at various temperatures. As a result, the data of each run of both the static-frequency and dynamic-frequency measurements had to be reduced to their equivalent at a common temperature. This conversion was accomplished by using a temperature-adjustment coefficient derived from the Van Vleck-Weisskopf theoretical equation. The intensity was assumed to vary according to $\frac{\gamma_{T_o}}{\gamma_T} = \left(\frac{T}{T_o}\right)^2$ at line-center frequency and to approach $\frac{\gamma_{T_o}}{\gamma_T} = \left(\frac{T}{T_o}\right)^4$ at a frequency of $5\Delta\nu$ or greater on either side of the line-center frequency, where

γ_{T_o} = attenuation in db/km at temperature T_o

γ_T = attenuation in db/km at temperature T.

Implied in these expressions is the assumption that $\Delta\nu$ is proportional to T^{-1}.

Since 27°C approximately represents the mean of the two extreme measuring temperatures, a temperature of 300°K was chosen as the temperature to which the data was adjusted. The adjustment coefficient was applied to each measured value of attenuation obtained by the fixed-frequency measuring technique, such that no additional adjustment was necessary for $\Delta\nu$ at each pressure. The peak intensity of the line at various pressures, obtained from the swept-frequency measurements, was adjusted to a value associated with the common temperature of 300°K by assuming

the peak intensity to be inversely proportional to the square of the temperature. The line width data obtained by the swept-frequency technique were temperature-adjusted, independently of the adjustment of the peak intensity, by applying the empirical relationship $\frac{\Delta\nu_{T_o}}{\Delta\nu_T} = \left(\frac{T}{T_o}\right)^{0.9}$ as measured by Hill and Gordy.[13] The exact temperature dependence of $\Delta\nu$, however, is uncertain. Although kinetic theory predicts the exponent to be $\frac{1}{2}$, experiments by Hill and Gordy,[12, 13] Howard and Smith,[14] and Beringer and Castle[7] indicate that the exponent is more nearly unity. Much experimental work on the temperature dependence of microwave absorption effects is still necessary.

In the analysis of this data, the value of the line-center frequency was taken to be 118.745 Gc, as measured by Anderson, Johnson, and Gordy,[2] and the mean value of the experimental data was chosen as representative of the measurements.

The Van Vleck-Weisskopf shape factor was assumed to adequately describe the shape of this spectral line. It was then necessary to determine the required constants of the shape factor in order to best describe the experimental data over the entire range of pressures from 8 mm to 760 mm Hg. The assumed expression for attenuation in db/km is as follows:

$$\gamma = K_o \nu^2 \left[\frac{\Delta\nu}{(\nu_o - \nu)^2 + (\Delta\nu)^2} + \frac{\Delta\nu}{(\nu_o + \nu)^2 + (\Delta\nu)^2} \right]$$

where γ = attenuation in db/km for 100% oxygen at 300°K

ν_o = line-center frequency in Gc (118.745 Gc)

ν = frequency in Gc

$\Delta\nu$ = half-intensity, half-width of the line in Gc

K_o = a constant for a given pressure and temperature (related to peak intensity and $\Delta\nu$ by $K_o \cong \frac{(\gamma \text{ peak})(\Delta\nu)}{\nu_o^2}$)

$$K_o = C\frac{P}{T^3}.$$

The CDC 1604 digital computer was used to make five complete calculations of attenuation at all pressures of interest for selected values of $\Delta\nu$ and K_o. The curves which best fit the experimental data at all measured pressures were calculated using assumed values of K_o, with its associated pressure and temperature dependence, and deriving values of $\Delta\nu$ from the measured peak intensity. Thus, the computed curves accomplished the necessary averaging and weighting of the experimental data at all pressures. The calculated curves for several pressures are shown in Figures 9 through 11. The experimental points shown on the curves were in all cases, except in the extreme frequencies located 4000 Mc on either side of the line, within the root-mean-square experimental accuracy of the data.

The empirical equation derived from the best fit of the experimental data is as follows:

$$\gamma = 24.9\frac{P}{T^3}\nu^2\left[\frac{\Delta\nu}{(118.745-\nu)^2+(\Delta\nu)^2} + \frac{\Delta\nu}{(118.745+\nu)^2+(\Delta\nu)^2}\right]$$

where γ = attenuation in db/km for 100% oxygen

P = absolute pressure in mm Hg (8 mm Hg to 760 mm Hg)

T = temperature in degrees Kelvin (near 300°K)

ν = frequency in Gc

$\Delta\nu$ = half-intensity, half-width of the line in Gc.

It is obvious from this expression that, for pure oxygen at 300°K, $K_o = 9.22 \times 10^{-7} P$ and that $\Delta\nu = \frac{0.0130\,P}{\gamma_{peak}}$ where γ_{peak} is the peak attenuation in db/km. The experimental value of C of 24.9 is in excellent agreement with the calculated value of 25.0.[27]

The curve of $\Delta\nu$ versus pressure in Figure 12 was derived using the average value of $\Delta\nu$ obtained from the calculated curves representing the best fit of the data. The slope of this line, $\frac{\Delta\nu}{P}$, is 1.90 Mc/mm Hg. Figure 13 shows the measured values of peak intensity versus pressure over the same pressure range.

The swept-frequency line-width data, shown in Figure 14, indicate a pressure-normalized line-width parameter of $\frac{\Delta\nu}{P} = 2.08$ Mc/mm Hg. The difference between this slope (2.08 Mc/mm Hg) and the slope of Figure 12 (1.90 Mc/mm Hg) is a measure of the experimental uncertainty. The difference between these two slopes is within the experimental error of the measurements.

Measurements of half-intensity half-widths in access of approximately 8.5 Mc by the frequency-scanning technique are restricted by the IF center frequency of 30 Mc and by transmitter frequency deviations of the transmitted signal. The distortion caused by these limitations is obvious in

Figure 14. This distortion becomes significant at a line width corresponding to a pressure of approximately 4 mm Hg. Thus, the data from 4.5 mm Hg to 6 mm Hg are not heavily weighted in the analysis, although the data photographs did not clearly indicate that the data should be discarded.

Although the fixed-frequency measurements represent slightly more experimental confidence than the swept-frequency data, a weighting factor for this data would be entirely arbitrary. Hence, in determining a most probable slope for the entire pressure range, much information is contained in the mean of these measurements. The mean slope is 1.99 Mc/mm Hg at 300°K. This value is in excellent agreement with the value of 1.97 Mc/mm Hg at 300°K measured by Hill and Gordy.[13] It is also in good agreement with the theoretical value of 2.064 Mc/mm Hg calculated by Artman and Gordon,[4] with the swept-frequency measurement being closer to this theoretical value.

Atmospheric propagation measurements at frequencies below line-center frequency made by this Laboratory[25] indicate a line-breadth constant of 0.045 cm^{-1}/Austin Atmosphere or 1350 Mc at a pressure of approximately 740 mm Hg. This data implies a line-width parameter of 1.825 Mc/mm Hg for air of temperature centered at 291°K. If this value is extrapolated to its sea level equivalent, a line width of 1.35 Gc at 300°K is expected. If the experimental data shown in Figure 10 for a pressure of 760 mm Hg are used alone to measure a value of $\Delta\nu$, then this value would be 1.40 Gc. The agreement between these two measurements supports the argument that $N_2 - O_2$ collisions and $O_2 - O_2$ collisions cause an equivalent amount of pressure broadening.[6, 19, 29]

Consider the value of 0.12 cm^{-1}/atmosphere at T = 193°K reported by Anderson, Johnson, and Gordy.[2] If $\Delta\nu$ is assumed to be proportional to T^{-1}, then the 0.12 cm^{-1}/atmos. at 193°K is equivalent to 2.32 Gc at 760 mm Hg and 300°K. Since this value is entirely too large, the temperature dependence of $\Delta\nu$ merits examination. If the data of Figure 12 is used to obtain a value for $\Delta\nu$ at 760 mm Hg and 300°K, then an exponent of the temperature ratio can be determined. Thus,

$$\frac{\Delta\nu_{300}}{\Delta\nu_{193}} = \left(\frac{193}{300}\right)^{x} = \frac{1.44}{3.6}$$

$$x = 2.08$$

This exponent is definitely higher than any predicted or measured value. The accuracy of the value of $\Delta\nu$ measured by Anderson, et al, is therefore questioned, as they mention, because of the "low intensity of the line."

Measurements of the 5-mm wavelength oxygen lines by Artman and Gordon,[4] Gokhale and Strandberg,[10] Zimmerer and Mizushima,[32] Stafford,[21] and others,[13, 3] indicate a range of values from 0.83 Mc/mm Hg to 2.23 Mc/mm Hg for the line-width parameter of these lines, the exact value being dependent upon the energy transition involved. Thus, the values of 1.90 and 2.08 Mc/mm Hg are within the range of values expected for an oxygen absorption line.

Very few measurements have been made of the peak intensity of this oxygen absorption line. Atmospheric propagation measurements by this Laboratory yield a peak intensity of 1.71 db/km for air of mean temperature

approximately 291°K.[25] Assuming the atmospheric gases to be composed of 21% oxygen, this value yields 7.66 db/km for the peak intensity of the line in pure oxygen at 300°K as compared with the value from Figure 13 of approximately 7.0 db/km. The uncertainty associated with the atmospheric propagation measurements is such that the data could be adequately described using a larger $\Delta\nu$ and a smaller peak intensity. Such a description would place the measurement in very close agreement with that of this investigation.

The slight increase in the measured intensity, a change of approximately 0.5 db/km over the pressure range from 3.5 mm Hg to 500 mm Hg, is attributed to the attenuation associated with the wings of the 5-mm oxygen lines. From the calculated curves of Figure 1, this effect at 290°K is expected to be approximately 0.30 db/km over this pressure range for 100% oxygen. Thus, within the limits of the experimental uncertainty of the measurements, pressure broadening of the 5-mm oxygen line complex accounts for the measured increase in peak attenuation.

Several explanations exist for the experimental data in the wings of the line being higher than predicted by the Van Vleck-Weisskopf shape factor. The explanations are associated with the assumed temperature-adjustment coefficients, spectral absorption lines of ozone, measuring uncertainty, and inadequacy of the shape factor. The values of attenuation measured in the wings of the line at 114.745 Gc and 122.745 Gc were of the order of magnitude of the uncertainty due to system noises.

At 114.745 Gc, the gas temperatures of 19.0°, 42.2°, and 35.0°C were quite remote from the chosen common temperature of 27°C; hence, temperature adjustment of the data involved coefficients considerably different from unity as a result of the T^{-4} variation in attenuation. The attenuation associated with this frequency is significantly changed from the measured value by the T^{-4} assumed variation.

Static-frequency measurements at a frequency of 122.745 Gc were taken for a gas temperature of approximately 285°K; hence, a temperature-adjustment coefficient considerably less than unity had to be used to obtain a value equivalent to the attenuation at 300°K. However, an inappropriate temperature adjustment would not, in itself, explain the discrepancy between the measured data and the calculated curve at this point.

Unlike the poor fit of the lower-frequency wing measured data to the calculated line shape at only one frequency, discrepancies between the measured points and the calculated curve on the high-frequency wing of the line were observed at several different frequencies as the pressure was reduced.

It is probable that the Van Vleck-Weisskopf shape factor does not exactly describe the line shape of this oxygen absorption line.[29] Evidence supporting this statement is the smooth curve formed by the experimental points which cannot be described exactly by the Van Vleck-Weisskopf shape factor as well as the failure of the shape factor to predict the narrow peak intensity section of the measured absorption curves at each pressure.

If the shape factor is calculated to fit the peak intensity section of the measured curves, it fails to fit the wings, and vice versa. Failure of the shape factor to describe the wings of water vapor and ammonia absorption is noted and discussed by Townes and Schawlow.[28d] Thus, the best description of the experimental data using the Van Vleck-Weisskopf shape factor represents a compromise between a description of the measured attenuation in the vicinity of the peak intensity and a description of the measured wings of the line.

Examination of the fixed-frequency instrumentation reveals that the largest probability for experimental error in the value of a data point lies in the higher pressure data. These errors are associated with the low-frequency noise or drift of the system. The data for the higher pressures represent the longest elapsed time between the calibration of the recorder and the recording of the data. Hence, the measured attenuation at the higher pressures is subject to the largest probability of error due to low-frequency noise. Runs of data were completed in the shortest possible time in order to reduce the probability of drift and to prevent the occurrence of large changes in the temperature of the absorption cell.

The accuracy of the swept-frequency measurements is limited largely by the narrow bandpass of the display oscilloscope and the accuracy to which the data can be obtained from the photographs. Of these two possible sources of error, data interpretation is the larger. To reduce this error, the data were interpreted several times each by two experimenters. Sources

of broadening other than pressure broadening were considered negligible in accord with the calculations shown in the appendix.

The accuracy to be expected of all the data is best described by stating that the calculated Van Vleck-Weisskopf curves shown in Figures 9 through 11 lie within the expected experimental accuracy. The largest discrepancies are associated with data at 114.745 Gc, in the vicinity of the peak intensity of the line, and in the high-frequency wings of the line.

Data taken with this system using air show the Air/0_2 broadening ratio to be approximately unity and the Air/0_2 attenuation intensity ratio to be approximately 0.21. Thus, the approximate horizontal attenuation in the atmosphere due to oxygen absorption can be obtained by multiplying the values of the absorption given here for pure oxygen by 0.21. The Van Vleck-Weisskopf equation representing horizontal atmospheric absorption due to the 2.53-mm wavelength oxygen absorption line for a dry atmosphere, as extrapolated from these measurements, is

$$\gamma = 5.23 \frac{P}{T^3} \nu^2 \left[\frac{\Delta\nu}{(118.745 - \nu)^2 + (\Delta\nu)^2} + \frac{\Delta\nu}{(118.745 + \nu)^2 + (\Delta\nu)^2} \right]$$

where $\Delta\nu = 1.9 \times 10^{-3} P$ for P = pressure in mm Hg ($4\,\text{mm} < P \leq 760\,\text{mm}$)

$\Delta\nu = 2.08 \times 10^{-3} P$ for P = pressure in mm Hg ($P \leq 4\,\text{mm}$)

for temperatures near 300°K.

A significant improvement in the instrumentation could be obtained by controlling the temperature of the absorption cell. This would prevent

expansion and contraction of the cell due to temperature changes during a measurement and would allow the attenuation as a function of gas pressure and frequency to be measured at constant values of temperature. Since the absorption of energy by oxygen is essentially a function of three variables (pressure, frequency, and temperature), controlling the temperature of the gas would also provide a means of measuring the change in attenuation as a function of temperature and frequency for constant values of pressure.

Placing the antennas at a greater distance from the teflon windows, increasing the center-frequency of the IF amplifier, and raising the power level of the transmitter could also improve the measuring capacity of the system.

IX. CONCLUSIONS

Although the Van Vleck-Weisskopf shape function does not exactly describe the shape of the 2.53-mm wavelength oxygen absorption line, it is a good approximation of the shape except in the far wings.

The shape of the absorption line as measured is best described for pressures from 8 mm Hg to 760 mm Hg by the equation

$$\gamma = 24.9 \frac{P}{T^3} \nu^2 \left[\frac{\Delta\nu}{(118.745 - \nu)^2 + (\Delta\nu)^2} + \frac{\Delta\nu}{(118.745 + \nu)^2 + (\Delta\nu)^2} \right]$$

for 100% oxygen near 300°K.

The measured line-width parameter, $\Delta\nu$, is best described by

$$\frac{\Delta\nu}{P} = 2.08 \text{ Mc/mm Hg} \quad \text{For} \quad P \leq 4 \text{ mm Hg}$$

$$\frac{\Delta\nu}{P} = 1.90 \text{ Mc/mm Hg} \quad \text{For} \quad 4 \text{ mm Hg} < P \leq 760 \text{ mm Hg}$$

$$\frac{\Delta\nu}{c} = 0.0481 \text{ cm}^{-1}/\text{atmos.}$$

for 100% oxygen at 300°K.

The measured peak intensity of the line is adequately describable as increasing only very slightly with pressure from a value of 6.5 db/km at 3.5 mm Hg to 7.0 db/km at 500 to 760 mm Hg for 100% oxygen at a temperature of 300°K.

BIBLIOGRAPHY

1. Anderson, P. W., "Pressure Broadening in the Microwave and Infrared Regions," Physical Review, Vol. 76, No. 5, September 1, 1949, pp. 647-661.

2. Anderson, Roy S., Charles M. Johnson, and Walter Gordy, "Resonant Absorption of Oxygen at 2.5-Millimeter Wavelength," Physical Review, Vol. 83, No. 5, September 1, 1951, pp. 1061.

3. Anderson, Roy S., William V. Smith, and Walter Gordy, "Line-Breadths of the Microwave Spectrum of Oxygen," Physical Review, Vol. 87, No. 4, August 15, 1952, pp. 561-568.

4. Artman, J. O., and J. P. Gordon, "Absorption of Microwaves by Oxygen in the Millimeter Wavelength Region," Physical Review, Vol. 96, No. 5, December 1, 1954, pp. 1237-1245.

5. Barrett, A. H., "Spectral Lines in Radio Astronomy," Proceedings of the IRE, Vol. 46, No. 1, January 1958, pp. 250-259, (a)p. 257.

6. Beringer, Robert, "The Absorption of One-Half Centimeter Electromagnetic Waves in Oxygen," Physical Review, Vol. 70, Nos. 1 and 2, July 1 and 15, 1946, pp. 53-57.

7. Beringer, Robert, and J. G. Castle, Jr., "Microwave Magnetic Resonance Spectrum of Oxygen," Physical Review, Vol. 1, January 1, 1951, pp. 82-88.

8. Cleeton, C. E., and N. H. Williams, "Electromagnetic Waves of 1 Cm Wave-Length and the Absorption Spectrum of Ammonia," Physical Review, Vol. 45, February 16, 1934, pp. 234-237.

9. Dicke, Robert H., Robert Beringer, Robert L. Kyhl, and A. V. Vane, "Atmospheric Absorption Measurements with a Microwave Radiometer," Physical Review, Vol. 70, Nos. 5 and 6, September 1 and 15, 1946, pp. 340-348.

10. Gokhale, B. V., and M. W. P. Strandberg, "Line Breadths in the 5-mm Microwave Absorption of Oxygen," Physical Review, Vol. 84, No. 4, November 15, 1951, p. 844L.

11. Gordy, Walter, William V. Smith, and Ralph F. Trambarulo, Microwave Spectroscopy, John Wiley and Sons, Inc., New York, 1953, (a) p. 5.

12. Hill, Robert M., and Walter Gordy, "Temperature Dependence of the Line Breadths of Oxygen," Physical Review, Vol. 91, No. 1, July 1, 1953, p. 222A.

13. Hill, Robert M., and Walter Gordy, "Zeeman Effect and Line Breadth Studies of the Microwave Lines of Oxygen," Physical Review, Vol. 93, No. 5, March 1, 1954, pp. 1019-1022.

14. Howard, R. R., and W. V. Smith, "Microwave Collision Diameters - I. Experimental," Physical Review, Vol. 79, No. 1, July 1, 1950, pp. 128-131.

15. Illinger, K. H., "Dispersion and Absorption of Microwaves in Gases and Liquids," Progress in Dielectrics, Vol. 4, Heywood and Company, Ltd., London, 1962, pp. 39-69.

16. Ingram, D. J. E., Spectroscopy at Radio and Microwave Frequencies, Butterworth's Scientific Publications, London, 1955, (a) p. 71, (b) p. 110.

17. Margenau, Henry, "Statistical Theory of Pressure Broadening," Physical Review, Vol. 82, No. 2, April 15, 1951, pp. 156-158.

18. Mizushima, Masataka, and Robert M. Hill, "Microwave Spectrum of O_2," Physical Review, Vol. 93, No. 4, February 15, 1954, pp. 745-748.

19. Purcell, E. M., "Measurement of Atmospheric Absorption," Propagation of Short Radio Waves, M. I. T. Radiation Laboratory Series No. 13, McGraw-Hill Book Co., Inc., New York, 1951, pp. 664-671.

20. Sheridan, J., "Microwave Spectroscopy of Gases," Progress in Dielectrics, Vol. 4, Heywood and Company, Ltd., London, 1962, pp. 3-36, (a) p. 12.

21. Stafford, Lannon F., "Spectroscopic Measurement of Oxygen Absorption Line Shape," Master's Thesis, The University of Texas, 1963.

22. Stitch, M. L., "Microwave Interaction with Matter," Proceedings of the IRE, Vol. 50, No. 5, May, 1962, pp. 1225-1231.

23. Straiton, A. W., and C. W. Tolbert, "Anomalies in the Absorption of Radio Waves by Atmospheric Gases," Proceedings of the IRE, Vol. 48, No. 5, May, 1960, pp. 898-903.

24. Sullivan, II, Roy S., "Atmospheric Absorption of Radio Signals of from 58 to 62 Kilomegacycles per Second," Master's Thesis, The University of Texas, January, 1963.

25. Tolbert C. W., C. O. Britt, and J. H. Douglas, "Radio Propagation Measurements in the 100 to 118 kMc/Sec Spectrum," Electrical Engineering Research Laboratory Report No. 107, The University of Texas, April 15, 1959.

26. Tolbert, C. W., and R. M. Dickinson, "Calculated Values of Absorption due to Water Vapor and Oxygen in the Millimeter Spectrum," Electrical Engineering Research Laboratory Report No. 6-42, The University of Texas, February 20, 1961.

27. Tolbert, C. W., and A. W. Straiton, "Synopsis of Attenuation and Emission Investigations of 58 to 62 kMc/s Frequencies in the Earth's Atmosphere," submitted to IEEE for publication.

28. Townes, C. H., and A. L. Schawlow, Microwave Spectroscopy, McGraw-Hill Book Co., Inc., New York, 1955.
(a) p. 336, (b) p. 337, (c) p. 374, (d) p. 347.

29. Van Vleck, J. H., "The Absorption of Microwaves by Oxygen," Physical Review, Vol. 71, No. 7, April 1, 1947, pp. 413-424.
(a) p. 415, (b) p. 415, (c) p. 418.

30. Van Vleck, J. H., and Henry Margenau, "Collision Theories of Pressure Broadening of Spectral Lines," Physical Review, Vol. 76, No. 8, October 15, 1949, pp. 1211-1214.

31. Van Vleck, J. H., and V. F. Weisskopf, "On the Shape of Collision-Broadened Lines," Reviews of Modern Physics, Vol. 17, Nos. 2 and 3, April-July, 1945, pp. 227-236.

32. Zimmerer, R. W., and M. Mizushima, "Precise Measurement of the Microwave Absorption Frequencies of the Oxygen Molecule and the Velocity of Light," Physical Review, Vol. 121, No. 1, January 1, 1961.

APPENDIX A

CALCULATIONS OF DOPPLER BROADENING AND WALL-COLLISION BROADENING OF LINE WIDTH

Doppler Broadening:

$$\Delta\nu = \frac{\nu_o}{c}\sqrt{2k\,N_o\,\ell n 2}\sqrt{\frac{T}{M}} = 3.58\times10^{-7}\sqrt{\frac{T}{M}}$$

$$\nu_o = 1.1875\times10^{11} \text{ c.p.s.}$$

$$T = 300\,^\circ K$$

$$M = 32 \qquad \text{For } 0_2^{16}$$

$$\Delta\nu = (3.58\times10^{-7})(1.1875\times10^{11})\sqrt{\frac{300}{32}}$$

$$\Delta\nu = 130.1 \text{ kc.}$$

Wall-Collision Broadening:

$$\Delta\nu = \frac{S}{V}\sqrt{\frac{RT}{8\pi^3 M}}$$

$$R = 8.31\times10^{7} \text{ erg/mole} \cdot {}^\circ K$$

$$\Delta\nu = 579\,\frac{S}{V}\sqrt{\frac{T}{M}} \text{ c.p.s. in c.g.s. units}$$

$$S = \pi DL = \frac{\pi L}{2} \text{ ft}^2$$

$$V = \pi\left(\frac{D^2}{4}\right)L = \frac{\pi L}{16} \text{ ft}^3$$

$$\frac{S}{V} = 8 \text{ ft}^{-1} = 0.262 \text{ cm}^{-1}$$

$$M = 32 \qquad \text{For } O_2^{16}$$

$$T = 300°K$$

$$\Delta\nu = (579)(0.262)\sqrt{\frac{300}{32}}$$

$$\Delta\nu = 464 \text{ c. p. s.}$$

APPENDIX B

ANTENNA PLACEMENT CALCULATIONS

For f = 120 Gc:

Assume a point source

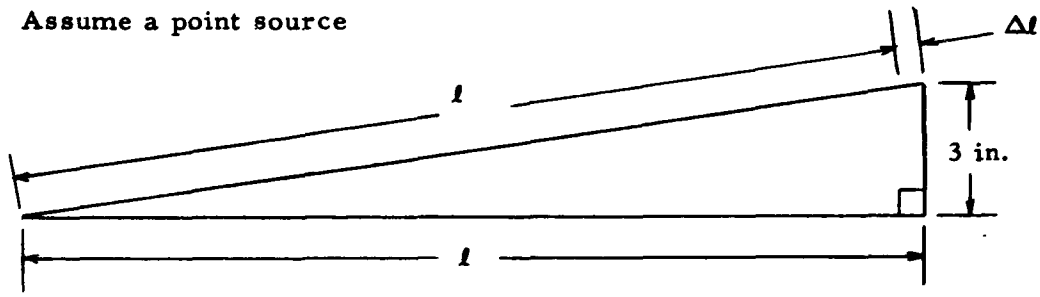

ℓ = distance from antenna to absorption cell

Make $\Delta\ell \leq \frac{\lambda}{8}$

$$\lambda = \frac{3 \times 10^{11}}{1.2 \times 10^{11}} = 2.5 \text{ mm} = 0.0984 \text{ in.}$$

$$\frac{\lambda}{8} = 0.0123 = \Delta\ell_{max.}$$

$$\ell^2 + (3)^2 = (\ell + \Delta\ell)^2$$

$$(\Delta\ell)^2 + 2\ell\Delta\ell - 9 = 0$$

$$\ell = \frac{9 - (\Delta\ell)^2}{2\Delta\ell} = \frac{9 - (0.0123)^2}{0.0246}$$

$$\ell = 366 \text{ in.} = 30.5 \text{ ft.}$$

$$\ell_{min.} = 30.5 \text{ ft.}$$

APPENDIX C

CALIBRATION OF SINUSOIDAL FREQUENCY SCALE

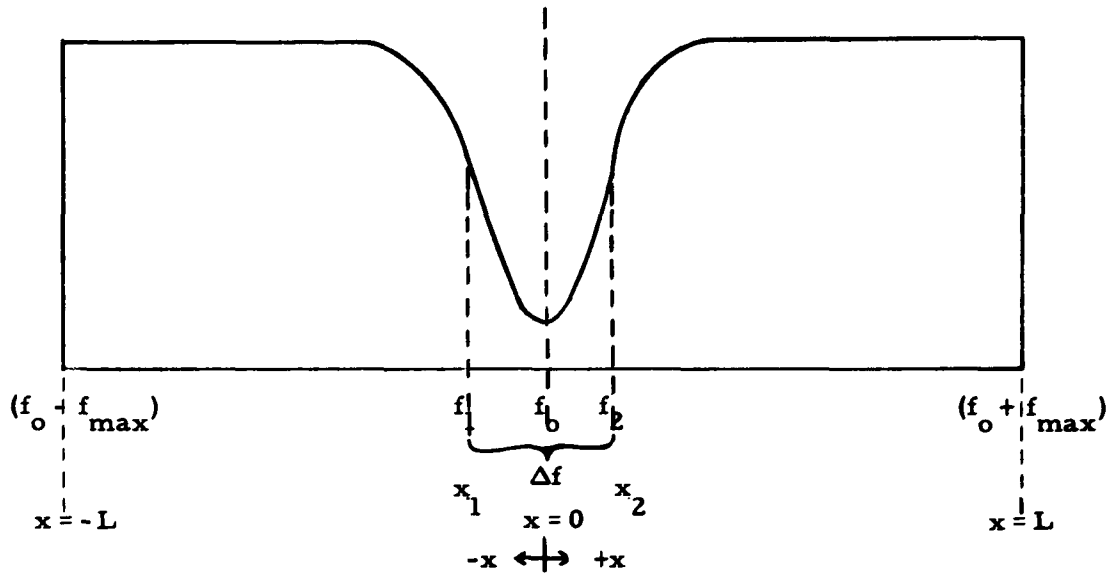

Frequency of transmitter = $f = f_o + f_{max.} \sin \omega t$

at $t = 0$, $f = f_o$

Position of electron beam on oscilloscope

scale = $x = C_o t$ (linear sweep)

$t = C_1 x$ where $C_1 = \frac{1}{C_o}$

at $t = 0$, $x = 0$

Thus,

$$f = f_o + f_{max.} \sin C_1 \omega x$$

at $x = L$, $f = f_o + f_{max.}$

$x = -L$, $f = f_o - f_{max.}$

Therefore,

$$f = f_o + f_{max} \sin \frac{\pi x}{2L}$$

$$\frac{\partial f}{\partial x} = \frac{\pi}{2L} f_{max.} \cos \frac{\pi x}{2L}$$

at $x = 0$, $\frac{\partial f}{\partial x} = K$ (measured calibration constant in Mc/cm)

$$\left.\frac{\partial f}{\partial x}\right|_{x=0} = \frac{\pi}{2L} f_{max.} = K$$

or

$$f_{max.} = \frac{2LK}{\pi}$$

Now,

$$f = f_o + f_{max.} \sin \frac{\pi x}{2L}$$

$$f = f_o + \frac{2LK}{\pi} \sin \frac{\pi x}{2L}$$

$$\Delta f = f_2 - f_1$$

$$f_1 = f_o + \frac{2LK}{\pi} \sin \frac{\pi x_1}{2L}$$

$$f_2 = f_o + \frac{2LK}{\pi} \sin \frac{\pi x_2}{2L}$$

$$\Delta f = \frac{2LK}{\pi} \left(\sin \frac{\pi x_2}{2L} - \sin \frac{\pi x_1}{2L} \right)$$

AF 33(657)-8716

DISTRIBUTION LIST

	Attn:	No. copies
Defense Documentation Center Cameron Station Alexandria, Virginia - 22314		10
Hq., AFSC Andrews Air Force Base Washington 25, D. C.	SCTAE/Col. Schulte	1
Electronics Systems Division L. G. Hanscom Field Bedford, Mass.	ESRDE/Maj. John Hobson	1
Aeronautical Systems Division Wright-Patterson AFB, Ohio	ASRNCF-2	4 + 1 reprod.
	ASRNCF/Mr. Hill	1
	ASRNC/Mr. Stimmel	1
	ASRNG/Mr. R. J. Doran	1
	ASRNGE-2/Mr. Wm Harmon	1
	ASRNR, Mr. E. B. Woodford	1
	ASAPRL/Tech Doc Library	1
	ASRNCS-1/Mr. Bartlett	1
	ASRNE/Mr. Noble	1
	ASRNRS-4/Mr. Schoonover	1
Air Force Cambridge Research Laboratories Electronics Research Directorate L. G. Hanscom Field Bedford, Mass.		1
Air University Maxwell AFB, Alabama	Library 7575	1
U. S. Naval Research Laboratory Washington 25, D. C.	Library	1
U. S. Army Signal Research and Development Laboratory Fort Monmouth, New Jersey	Technical Reports Library	1
Commanding Officer Harry Diamond Laboratories Washington 25, D. C.	Library	1
Commanding Officer U. S. Army Electronics Research and Development Activity White Sands Missile Range, New Mexico - 88002	SELWS-M, Chas. Querfeld	1
Collins Radio Company Cedar Rapids, Iowa	Mr. G. Phillips	1
Lincoln Laboratory, M. I. T. P. O. Box 73 Lexington 73, Mass.	Documents Library	1